

Research Article

A Comprehensive Analysis of the Changes in Precipitation Patterns over Beijing during 1960–2012

Xiaomeng Song ^{1,2,3}, Jianyun Zhang,² Chunhua Zhang,¹ and Xianju Zou¹

¹School of Resources and Geosciences, China University of Mining & Technology, Xuzhou 221116, China

²State Key Laboratory of Hydrology-Water Resources and Hydraulic Engineering, Nanjing Hydraulic Research Institute, Nanjing 210029, China

³State Key Laboratory of Water Resources and Hydropower Engineering Science, Wuhan University, Wuhan 430072, China

Correspondence should be addressed to Xiaomeng Song; xmsong.cn@gmail.com

Received 15 October 2018; Accepted 28 January 2019; Published 6 March 2019

Academic Editor: Efthymios I. Nikolopoulos

Copyright © 2019 Xiaomeng Song et al. This is an open access article distributed under the Creative Commons Attribution License, which permits unrestricted use, distribution, and reproduction in any medium, provided the original work is properly cited.

Precipitation pattern has changed over many regions in recent decades, which may cause the risk of flood or drought. In this study, the main objective is to evaluate the spatiotemporal variability of precipitation in Beijing from 1960 to 2012. First, the mean monthly, seasonal, and annual precipitation series were used to analyze the temporal variation using regression, Mann–Kendall (M-K) test, Sen's slope, and Pettitt tests. The results showed that the annual mean precipitation had a clear decreasing trend, with the statistically significant decrease in summer (especially in July and August) and significant increase in spring (especially in May). Although the decreasing trend is shown in the precipitation concentration indicators, the temporal uneven distribution of precipitation has unchanged. Subsequently, the precipitation time series at 30 stations over Beijing were used to evaluate the changes in precipitation pattern. The results showed that the annual series for the most rain gauges had decreasing trends with gradual changes. The spatial distribution of precipitation and other indices is geographically consistent, reflecting the principal physiographic and climatic conditions. At the same time, the effects of the terrain and urban development on the precipitation spatial distribution were detected. Generally, the large and heavy precipitations frequently occur in the plain areas, while the precipitation in the mountain areas is dominated by the small and medium precipitation. As a whole, the total precipitation in the plain areas (558.8 mm) was slightly higher than that in the mountainous areas (533.0 mm), while the precipitation in the urban areas (575.9 mm) was much higher than in the surrounding suburb areas (538.9 mm) during 1960–2012. The differences between the plain and mountainous areas during the period of 1960–1979, 1980–1999, and 2000–2012 were 24.2 mm, 32.6 mm, and 17.7 mm, respectively. The differences in precipitation between the urban and suburb areas for the three periods were 32.9 mm, 45.2 mm, and 31.0 mm, respectively, with the amount accounting for 5.51%, 7.66%, and 5.94% of the mean precipitation in the urban areas for the corresponding periods.

1. Introduction

The long-term observation of climatic variables as a practical approach for monitoring climate change is receiving considerable attention from researchers throughout the world. Of the common climatic variables, precipitation is the most changeable in time and space, which directly affects natural cycles of water resources. In addition, severe precipitation can also cause storm-induced floods [1] and heavy sediment loads from watersheds which may change sediment

transport in rivers and coastal waters. There is a growing concern in the scientific community over whether there are significant changes in precipitation amount, intensity, duration, and frequency because changes in precipitation patterns may lead to floods or droughts in different areas [2–4]. Also, trend and variability analysis of rainfall requires urgent and systematic attention because of significant possible influences on freshwater availability, occurrence of extreme events, food security, and economic activities [5–8]. Therefore, the spatial and temporal variability of

precipitation time series is important from both the scientific and practical point of view.

Linking with industrialization, during the late 20th to the early 21st century, urbanization occurred rapidly across developing countries, especially in China; this urbanization is projected to continue over the coming decades. Urbanization has modified the earth system [9] and local water cycle [10], creating environmental burdens, including urban heat islands (UHI) [11], urban aerosols [12], storm, and flooding in urban areas [13, 14]. As a result, it is important to analyze the rainfall variability in urban areas. Several studies have addressed issues related to urban heat island, impact of urbanization on rainfall, and spatiotemporal variations of rainfall, especially for the metropolitan areas [3, 4, 15–19]. Urban expansion is associated commonly with increased amount of precipitation and the frequency of extreme precipitation in urban areas as well as downwind areas because of the effect of urban heat island and high concentrations of anthropogenic aerosols [20–22]. Precipitation changes and variability in the metropolitan areas could present a challenge in terms of stormwater management, water quality, and water supply [23, 24].

Beijing, located in northern China and surrounded by mountains with complex terrain, is the capital of China and one of the most populous cities in the world. It has experienced rapid urbanization in the past few decades due to China's reforms [25]. The built-up area of Beijing has grown from 346 km² in 1980 to 1350 km² in 2013, and the resident population of the city has exceeded 21 million. The complex terrain is likely to cause valley wind circulation, which may have an impact on the local climate, and the changes in the underlying characteristics as a result of rapid urbanization will also influence local precipitation. Therefore, the study of temporal and spatial variations in the local climatic characteristics of Beijing is important to our understanding of the impacts of urbanization on the local climate. To date, numerous studies have analyzed rainfall variability at different temporal scales from different perspectives. Other studies have been done on the possible effects of urban expansion on precipitation in the Beijing areas [3, 17, 19, 25–32]. For example, Miao et al. [29] discussed the effects of land use or land cover on the characteristics of boundary layer structures of urban areas. Their results showed that the urban-rural circulations induced by topographic differences were one of the important causes for the prevalence of mountain-valley flows in the Beijing area. Zhang et al. [33] found that urbanization predominantly contributed to a reduction in precipitation in Beijing, based on a mesoscale model, particularly over the Miyun reservoir area. Because Beijing has a varied and complex topography with high mountains in the west and north parts of Beijing, Sun et al. [34] and Wu et al. [35] pointed out that the terrain had an important effect on the location and distribution of precipitation. Similarly, Sun and Yang [36] found that a reduction in rainfall was caused by the joint effects of topography and the urban heat island. In addition, significant spatiotemporal and interseasonal variations in the trends and variability of precipitation in the Beijing area were noticed. For example, Li et al. [15] revealed that there was an

increasing trend from 1724 to 2009; in addition, they found some periodic characteristics that affected the trends regarding the amount of annual precipitation. Zhai et al. [4] discussed the spatiotemporal variation of precipitation from 1724 to 2010 based on the same meteorological station. The annual precipitation presented a slowly increasing trend during 1724–2010, which is consistent with that of the work by Li et al. [15]. Further, Zhai et al. [4] discussed the spatial variations of precipitation from 1980 to 2010 based on the 20 weather stations and showed that annual precipitation had decreased significantly during the first decade of the 21st century compared to the last two decades of the 20th century.

For this study, a comprehensive analysis was conducted of the changes in precipitation at the regional-scale using 30 rain gauges in the Beijing metropolitan area. This work attempted to (1) identify gradual trends and abrupt shifts at various temporal scales (monthly, seasonal, and annual) in precipitation data series, (2) investigate the temporal and spatial variations of precipitation with the consideration of the urbanization and topography effect, and (3) discuss the changes of precipitation patterns based on the classified precipitation events. The findings may be helpful to scientifically understand the structural changes in precipitation and to evaluate the water availability and urban water resources management in the study area. This study can also provide a reference for further studies on precipitation mechanisms in urban areas.

2. Materials and Methods

2.1. Data Sources and Data Preprocessing. The daily rain gauge data from 30 stations in Beijing areas were analyzed in this study. These data were provided by the Beijing Hydrological Stations (BHS) of the Beijing Water Authority (BWA). Note that most of the 30 observation stations within Beijing were established in the late 1950s and early 1960s and formed a fixed network by the end of 1960s. As a result, the precipitation data from 1960 to 2012 are used to analyze the spatial distribution and the urbanization effects. The locations are shown in Figure 1, and details about these stations are listed in Table 1. For some stations, the missing precipitation due to disruption in data collection requires data infilling. Various infilling methods have been reported in the literature, such as nearest neighbor, inverse distance, linear regression, ordinary kriging, multiple linear regression, neural networks, and copula-based method [37, 38]. Compared to infilling precipitation data on short time scales (up to several days), the annual time scale is relatively simple. As a result, in this work, the nearest neighbor method is used to infill the missing data via the neighbor control station and its observations. The missing data can be estimated by multiplying with the ratio of the long-term means of the target station and its nearest neighbor. In this study, the “nearest” neighbor station was selected based on the correlation coefficient and its sufficiently available precipitation series. For example, the four stations surrounding Gao-beidian are Tongzhou, Songlinzha, Youanmen, and Majuqiao. Figure 2 shows the annual precipitation correlation

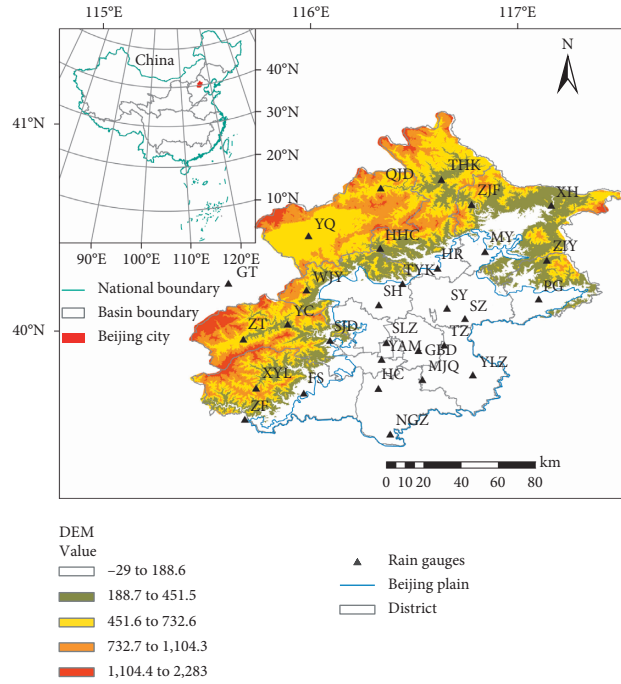


FIGURE 1: Location and the distribution of the 30 rain gauges in Beijing that were used in this study.

TABLE 1: Location of the 30 rain gauges and time series information.

Station	Abbreviation	Longitude (°E)	Latitude (°N)	Time series	Missing data
Fangshan	FS	115.97	39.70	1950–2012	1968, 1992–1996
Gaobeidian	GBD	116.52	39.91	1972–2012	None
Guanting	GT	115.61	40.23	1950–2012	None
Huangcun	HC	116.33	39.73	1954–2012	1960–1961
Huanghuacheng	HHC	116.34	40.40	1955–2012	None
Huairou	HR	116.61	40.31	1952–2012	None
Majuqiao	MJQ	116.55	39.76	1960–2012	1961
Miyun	MY	116.84	40.39	1950–2012	1962
Nangezhuang	NGZ	116.39	39.50	1965–2012	1976–1978
Pinggu	PG	117.10	40.16	1950–2012	1992
Qianjiadian	QJD	116.34	40.69	1961–2012	None
Shahe	SH	116.33	40.13	1959–2012	1979
Sanjiadian	SJD	116.10	39.96	1950–2012	None
Songlinzha	SLZ	116.37	39.95	1963–2012	None
Shunyi	SY	116.66	40.11	1950–2012	1992–1996
Suzhuang	SZ	116.75	40.06	1950–2012	None
Tanghekou	THK	116.63	40.73	1960–2012	1962
Taoyukou	TYK	116.45	40.23	1962–2012	None
Tongzhou	TZ	116.65	39.93	1950–2012	None
Wangjiayuan	WJY	115.98	40.20	1962–2012	None
Xiahui	XH	117.16	40.61	1961–2012	1970–1973
Xiayunling	XYL	115.74	39.73	1951–2012	1961, 1992–1996
Youanmen	YAM	116.35	39.87	1963–2012	1968
Yanchi	YC	115.89	40.03	1963–2012	None
Yulinzhuang	YLZ	116.79	39.79	1961–2012	None
Yanqing	YQ	115.99	40.46	1959–2012	1992–1993
Zhangfang	ZF	115.69	39.58	1963–2012	None
Zhangjiafen	ZJF	116.78	40.61	1960–2012	None
Zhenluoying	ZLY	117.14	40.34	1954–2012	None
Zhaitang	ZT	115.68	39.96	1951–2012	None

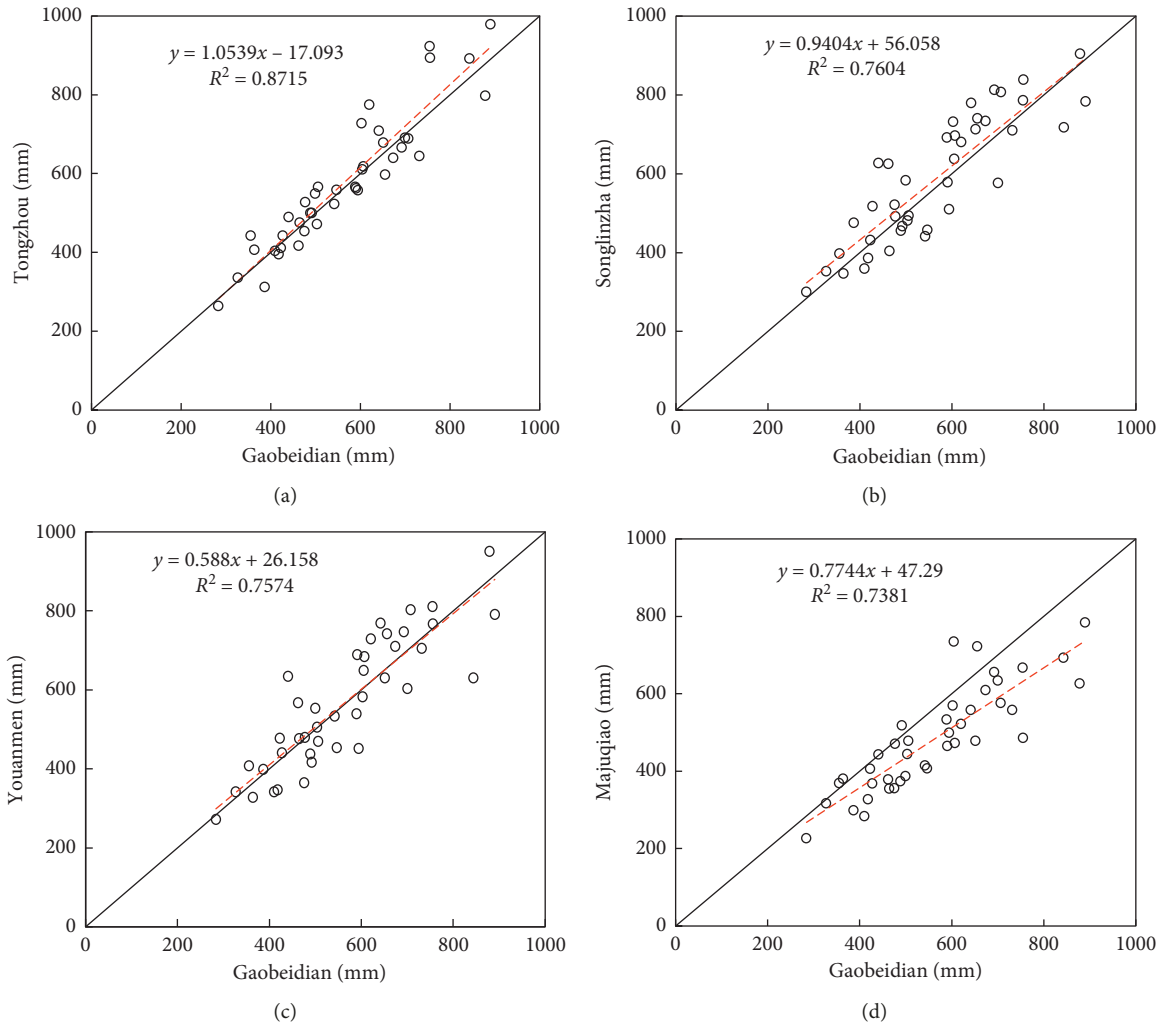


FIGURE 2: Scatter plots for the correlation relationship between Gaobeidian station and surrounding rain gauges. The black solid lines are 1 : 1 lines. The red dashed lines mean the linear regression lines.

relationships between Gaobeidian and other four stations. With highest correlation, Tongzhou station is the “nearest” neighbor station to infill the missing annual precipitation at Gaobeidian station. In addition, there is no missing precipitation data at Tongzhou station. Once the “nearest” neighbor station has been identified for each station with missing data, using the linear regression equation provided in Table 2, missing data can be infilled. From Table 2, we find that the precipitation series for the nearest neighbor stations are quite strongly correlated with those stations that have missing data; for most stations, correlation coefficients exceed 0.7.

2.2. Classification in Precipitation Grades and Subregions.

In this study, the standard for records is that precipitation amount is greater than or equal to 0.1 mm when rainfall occurs. To further understand the change of precipitation patterns over Beijing, the observed daily precipitation was categorized into four grades of intensity according to China Meteorological Administration (CMA) standards: small

($0.1 \text{ mm} \leq \text{daily precipitation} < 10 \text{ mm}$); medium ($10 \text{ mm} \leq \text{daily precipitation} < 25 \text{ mm}$); large ($25 \text{ mm} \leq \text{daily precipitation} < 50 \text{ mm}$); heavy ($50 \text{ mm} \leq \text{daily precipitation}$). We also define two indices to assess these changes in precipitation patterns according to the work from Song et al. [39]. One is precipitation incidence (PI), which means the proportion of precipitation days for every precipitation grade to the total days of precipitation in a year; the other is precipitation contribution (PC), which means the proportion of precipitation amount for every precipitation grade to the total amount of precipitation in a year.

Additionally, the rain gauge stations provide reasonably good coverage of different altitudinal zones, i.e., plain (including urban and suburb areas) and mountainous areas in the study area. By considering the complex surface characteristics, 30 observation sites were divided into two categories, plain and mountain areas (Figure 1). There are 18 sites (SLZ, YAM, GBD, TZ, HC, MJQ, SH, SY, SZ, YLZ, ZF, FS, SJD, TYK, HR, MY, PG, and NGZ) covering the plain areas and 12 sites covering the mountain areas. Among these stations in the plain areas, four stations located in urban area

TABLE 2: Information for infilling missing data.

Station	Nearest neighbor	Calibration series	Correlation coefficient	Equation
FS	ZF	1963–1967, 1969–1991, 1997–2012	0.78	$y = 0.849x + 61.5$
GBD	TZ	1972–2012	0.93	$y = 0.827x + 86.5$
HC	FS	1962–1967, 1969–1991, 1997–2012	0.68	$y = 0.537x + 225.8$
MJQ	TZ	1960, 1962–2012	0.83	$y = 0.738x + 65.4$
MY	ZLY	1960, 1963–2012	0.64	$y = 0.9x + 53.78$
NGZ	YLZ	1979–2012	0.72	$y = 0.657x + 87.1$
PG	ZLY	1960–1991, 1993–2012	0.66	$y = 0.519x + 172.2$
QJD	YQ	1961–1991, 1994–2012	0.69	$y = 0.569x + 173.4$
SH	SLZ	1963–1978, 1980–2012	0.80	$y = 0.673x + 160$
SLZ	TZ	1963–1967, 1969–2012	0.80	$y = 0.795x + 121.5$
SY	SZ	1960–1991, 1997–2012	0.83	$y = 0.831x + 80.8$
THK	HHC	1960–1961, 1963–2012	0.75	$y = 0.504x + 164.4$
TYK	SH	1962–1978, 1980–2012	0.71	$y = 0.713x + 203.1$
WJY	SH	1962–1978, 1980–2012	0.73	$y = 0.7682x + 125.5$
XH	MY	1963–1969, 1974–2012	0.75	$y = 0.570x + 267.2$
XYL	ZT	1960, 1962–1991, 1997–2012	0.77	$y = 1.203x + 72.4$
YAM	TZ	1963–1967, 1969–2012	0.82	$y = 0.814x + 89.7$
YC	ZT	1963–2012	0.82	$y = 0.892x + 67.5$
YLZ	TZ	1961–2012	0.85	$y = 0.861x + 24.2$
YQ	GT	1960–1991, 1994–2012	0.74	$y = 0.974x + 83.9$
ZF	FS	1963–1967, 1969–1991, 1997–2012	0.78	$y = 0.708x + 193.7$

(SLZ, YAM, GBD, and TZ) were used to estimate the mean precipitation in the urban areas and six surrounding stations (HC, MJQ, SH, SY, SZ, YLZ) were selected to calculate the corresponding mean precipitation in the suburb areas.

2.3. Precipitation Concentration Index, Concentration Degree, and Concentration Period. The precipitation concentration index (PCI) developed by Oliver [40] was used to explore the changing features of precipitation concentration in Beijing. PCI was proposed as an indicator of monthly rainfall heterogeneity, according to the following equation:

$$PCI = \frac{\sum_i^{12} P_i^2}{(\sum_i^{12} P_i)^2} \times 100, \quad (1)$$

where P_i is the monthly precipitation in month i . According to equation (1), the lowest theoretical value of PCI is 8.3, which means the perfect uniformity in precipitation distribution. Oliver [40] classified PCI values in four categories: (1) $PCI \leq 10$ means uniform precipitation distribution, i.e., low precipitation concentration; (2) $10 < PCI \leq 15$ means moderate precipitation concentration; (3) $15 < PCI \leq 20$ means irregular precipitation distribution, i.e., high precipitation concentration; and (4) $PCI > 20$ means strong irregular precipitation distribution, i.e., very high precipitation concentration.

In addition, the precipitation concentration degree (PCD) and the precipitation concentration period (PCP) proposed by Zhang and Qian [41] were also used to analyze the interannual variations of precipitation amounts. The basic principle for calculating the PCD and PCP is based on the vector of monthly total precipitation [42]. The assumptions can be made that monthly total precipitation is a vector quantity with both magnitude and that the direction

for a year can be seen as a circle (360°). Then, the yearly PCP and PCD for a location can be defined as follows:

$$P = \sum P_i,$$

$$P_x = \sum P_i \cdot \sin \theta_i,$$

$$P_y = \sum P_i \cdot \cos \theta_i, \quad (2)$$

$$PCP = \arctan\left(\frac{P_x}{P_y}\right),$$

$$PCD = \frac{\sqrt{P_x^2 + P_y^2}}{P},$$

where P_i is the monthly precipitation of the i th month, θ_i is the azimuth of the i th month, and P is the total precipitation amount. PCP can reflect which month the maximum monthly precipitation appears in. The corresponding relation between PCP and month in a year is as follows: January (0°), February (30°), March (60°), April (90°), May (120°), June (150°), July (180°), August (210°), September (240°), October (270°), November (300°), December (330°). PCD can reflect the degree to which annual total precipitation is distributed in 12 months, which is ranging from 0 to 1.

2.4. Trends Detecting Method. A trend analysis was performed to detect gradual changes or tendencies in the time series data, using the Mann–Kendall (M–K) test and Sen’s slope method. Both are commonly used tests for trend detection [43–51]. Trends were evaluated using the non-parametric M–K test [44, 45]. Significance of trend was evaluated at the 0.05 and 0.10 levels. The magnitude of trends

was evaluated using Sen's slope [46]. The M-K test and Sen's slope were chosen because they were widely used to detect the trends of hydrological and meteorological data time series. The details of the M-K test and Sen's slope are introduced in Appendix.

2.5. Pettitt Change Point Analysis. Nonstationarity in time series can also be characterized by abrupt shifts in the mean or variance of the series. To identify possible shifts, standard change-point procedures have been applied to multiple time series in Earth sciences including precipitation and temperature [52]. One type of homogeneity (change-point) test is the Pettitt test [53], which is a nonparametric test—requiring no assumption on the underlying distribution [54].

To perform the two-tailed hypothesis test on the location parameter (mean), the Pettitt test statistic is calculated as

$$D_{ij} = \begin{cases} -1, & x_i < x_j, \\ 0, & x_i = x_j, \\ 1, & x_i > x_j, \end{cases} \quad (3)$$

where x_i and x_j correspond to the magnitude of the hydroclimatic variable under consideration and x_i precedes x_j in time. For evaluation over the entire sample (T years), these D statistics are combined as follows:

$$U_{t,T} = \sum_{i=1}^t \sum_{j=t+1}^T D_{ij}. \quad (4)$$

The statistic U_t is equivalent to a Mann–Whitney statistic for testing that the two samples X_1, \dots, X_t and X_{t+1}, \dots, X_T come from the same population. The test statistic U_t is evaluated for all possible values of t ranging from 1 to T . The most probable year of a change-point occurring is evaluated using a two-tailed test on the following statistic:

$$K_T = \max |U_{t,T}|. \quad (5)$$

If the statistic K_T is significantly different from 0, then a change-point occurs in the year t corresponding to the point in time for which the largest absolute value of $U_{t,T}$, is obtained. The probability of a shift in a year where $|U_{t,T}|$ is the maximum is estimated by [55]

$$P = 2 \exp\left(\frac{-6K_T^2}{T^3 + T^2}\right). \quad (6)$$

Given a certain significance level α , if $P < \alpha$, we reject the null hypothesis and conclude that X_t is a significant change point at level α . The two significant levels ($\alpha = 0.05$ and $\alpha = 0.10$) were used in this work. In this study, the monthly, seasonal, and annual series of regional mean precipitation and the annual precipitation series for all the stations were used to detect the change points based on the Pettitt method.

3. Results and Discussion

3.1. Changes of Regional Mean Precipitation. As seen in Figure 3, the annual mean precipitation in Beijing areas

during 1960–2012 ranges from 383.9 mm (1965) to 797.9 mm (1964) with an average of 553.6 mm. The annual mean precipitation has a significantly decreasing trend at a rate of 11.6 mm/10a from 1960 to 2012, as analyzed by the linear regression method. For seasonal precipitation, the spring and autumn precipitations have a slightly increasing trend analyzed (4.7 mm/10a and 4.9 mm/10a); in contrast, summer precipitation has a visibly decreasing trend (21.1 mm/10a), which is greater than the decline rate in the annual precipitation series. Unlike the above three seasons, the trend of mean precipitation in winter has been almost flat, fluctuating within a range from 0.9 to 27.7 mm. Therefore, decreasing precipitation in summer has been the most important factor in the overall decrease of annual precipitation in Beijing. Several periods of severe droughts and moisture surpluses are evident in the anomaly series of regional mean precipitation in Figure 3. For example, the long-term dry period during 1999–2011 in Beijing is characterized by a high number of negative anomalies. Simultaneously, various temporal variations for interannual and interdecadal variability of seasonal precipitation were exhibited during 1960–2012 from the precipitation anomaly series and the 11-year moving-average series. For instance, in the period of 2000–2012, although the precipitation amount in certain years (2008 and 2012) is on the high side (larger than the mean value during 1960–2012), the summer total precipitation is relatively lower than its long-term mean. In contrast, the precipitation amount in spring and autumn in the most years during 2000–2012 is on the high side.

The M-K test and Sen's slope estimation were applied to detect the trends of the monthly, seasonal, and annual precipitation series during 1960–2012, as shown in Table 3. For the monthly scale, the series in May had a statistically significant increasing trend, while that in July and August had a significant decreasing trend, both at a level of $\alpha = 0.05$. The series in January and February had a significantly decreasing trend at a level of $\alpha = 0.10$. All other series had a nonsignificant trend at both levels during this study period. For the seasonal scale, the precipitation series in spring showed a significant increasing trend, while that in summer showed a statistically significant decreasing trend, both at a level of $\alpha = 0.05$. Both the precipitation series in autumn and winter had a nonsignificant trend. For the annual scale, there is a nonsignificant trend for the annual precipitation series during 1960–2012 at any level of $\alpha = 0.05$ or $\alpha = 0.10$.

The monthly variation of precipitation amounts is shown in Figure 4. The highest precipitation occurred in the wet season (May to October), especially in the period from June to September (namely flood season in Beijing), while the cold season (November to April) received less precipitation. The precipitation in the period from May to October accounted for 91.8% of the annual mean precipitation. Additionally, the precipitation in flood season contributed more than 81.5% to the annual mean precipitation. Further, it is clear that a large percentage of total precipitation occurs in summer, ranging from 39.5% to 87.4%, especially in July (8.3%–58.2%) and August (6.6%–50.6%). The maximum and minimum values for average monthly precipitation were

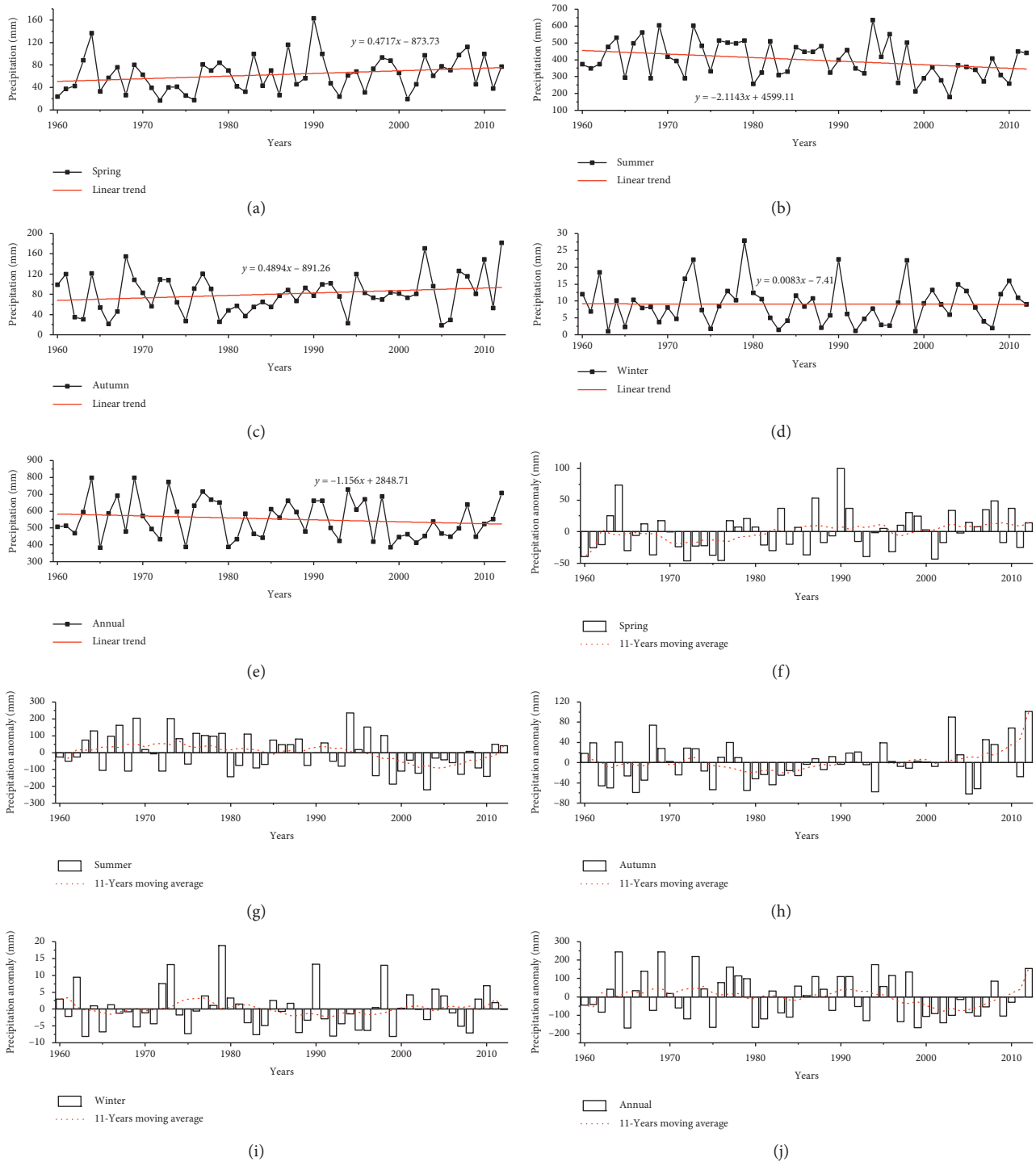


FIGURE 3: Time series of precipitation and anomaly in the Beijing metropolitan area from 1960 to 2012.

183.9 mm in July and 2.2 mm in December. To further discuss the variation of monthly precipitation, the time series of PCI, PCD and PCP are shown in Figure 5. As seen in Figure 5, the PCI in Beijing during 1960–2012 ranges from 13.1 (2003) to 37.4 (1962) with an average of 23.7. The PCD ranges from 0.47 (2003) to 0.86 (1994) with the mean of 0.72 over the period of 1960–2012. Overall, the precipitation over

Beijing has strongly uneven monthly precipitation distribution, where most precipitation occurred in summer, i.e., June, July, and August (as shown in Figure 4). Additionally, the PCI and PCD both have a slight decreasing trend at a rate of 1.68/10a and 0.02/10a from 1960 to 2012, as analyzed by the linear regression method. To some extent, the decreasing PCI (PCD) may be caused by the significant

TABLE 3: Trend test results of the monthly, seasonal, and annual precipitation during 1960–2012 tested by the M-K method and Sen's slope method. The uncertainty range covered from 5% to 95% between the minimum and maximum values of Sen's slope.

	Z value	Sen's slope (mm/a)	Minimum	Maximum
Jan	-1.695*	-0.009	-0.018	0
Feb	-1.918*	-0.043	-0.113	-0.007
Mar	-1.036	-0.055	-0.111	0.067
Apr	1.365	0.148	-0.060	0.265
May	2.179**	0.379	0.146	0.476
Jun	1.289	0.465	-0.375	0.724
Jul	-1.971**	-1.227	-2.200	-0.122
Aug	-2.148**	-1.401	-3.250	-0.892
Sep	0.905	0.248	-0.350	0.550
Oct	0.721	0.099	-0.225	0.207
Nov	0.744	0.037	-0.077	0.075
Dec	1.204	0.011	-0.005	0.033
Spring	2.086**	0.535	0.025	1.025
Summer	-2.202**	-2.150	-4.136	-0.344
Autumn	1.243	0.569	-0.304	1.250
Winter	0.184	0.007	-0.134	0.102
Annual	-0.767	-0.861	-3.159	1.344

Note. **Statistically significant trends at the 10% and 5% significance levels, respectively.

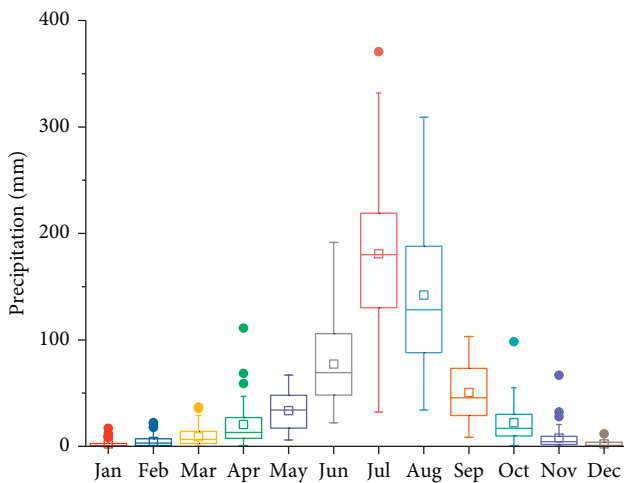


FIGURE 4: Box-plot for monthly precipitation amount during 1960–2012. The boxes indicate the 25th, 50th, and 75th percentiles and the whiskers indicate the values with maximum 1.5 interquartile ranges. The hollow square indicates the mean value. The solid circle means the outlier.

decreases in precipitation in summer and the increases in spring and autumn for the Beijing area (as shown in Figure 3). According to the changes of PCP in Figure 5, the range of the mean yearly PCPs in Beijing is 189 ± 7 , implying that annual precipitation mainly falls in summer (June–July–August). The time of the PCP mainly appears from the end of June (23, June) to the end of July (26, July). The maximum monthly precipitation in most years (46 years) occurs in July and the other occurs in June (7 years).

Change points in the monthly, seasonal, and annual series over Beijing were detected based on the Pettitt method. Then, the changes in the two samples before and

after the change point were examined, as shown in Table 4. Significant abrupt changes in monthly precipitation were found in May (47% upward in 1976) and August (46% downward in 1996) at a level of $\alpha = 0.05$. A significant abrupt change in monthly precipitation was also found in July (31% downward in 1998) at a level of $\alpha = 0.10$. Of them, as shown in Table 4, the significant downward change points occurred in the end of 1990s with the mean precipitation decreasing by 46% (1996) and 31% (1998), while the significant upward change point in the mid 1970s (1976) with the mean precipitation increasing by 47%. Other monthly precipitation series have no significant abrupt change during 1960–2012. For the seasonal scale, only summer precipitation has a significant abrupt change in 1996, and the downward magnitude is approximate 25% compared with the mean value of the entire series. Similar to the other three seasons, the annual precipitation has no significant abrupt change at either significant level.

3.2. Changes of Spatial Distribution of Precipitation Amount.

The spatial distribution of the annual precipitation and their trend test results is shown in Figure 6. As shown in Figure 6(a), it can be seen from this figure that the average annual precipitation varies greatly in Beijing and it varies from almost 400 mm in the west to more than 600 mm in the east. From the spatial perspective, the distribution shows that the precipitation is decreasing from east to west due to orographic influence. Apparently, the annual precipitation in the Beijing Plain is greater than in the mountainous areas. But the highest value of precipitation frequently occurred in the front belts (e.g., HR and MY stations) between the plain and mountainous areas. As a whole, there was one local maximum of precipitation with an annual mean precipitation of 650 mm, located in the vicinity of the Huairou and Miyun reservoirs in the northeastern section of Beijing. Another local maximum was centered at the XYL stations in the Fangshan district in the southwestern part of Beijing. With regard to the interannual variability of precipitation, the coefficient of variation and standard deviation of annual precipitation have been identified for the period of analysis, as shown in Figures 6(b) and 6(c). The range of values over Beijing is from 0.199 to 0.380. The lowest values appear in the northwestern area, and the highest values appear in the front belts between the plain and mountainous areas, which is similar to the spatial pattern of annual mean precipitation. The spatial distribution of the standard deviation in precipitation also shows the similar pattern to the annual precipitation. This explains the standard deviation (coefficient of variation) increases with the annual mean precipitation, namely, the higher the annual precipitation is, the higher the degree of uncertainty (standard deviation and coefficient of variation) is. This might increase the degree of uncertainty in the availability of regional water resources, due to the close relationship between the precipitation amount and the regional water resources.

The spatial distribution of Z values of the M-K trend test, Sen's slope, and linear trend for the individual rain gauges is also shown in Figure 6. The annual trends found by the linear

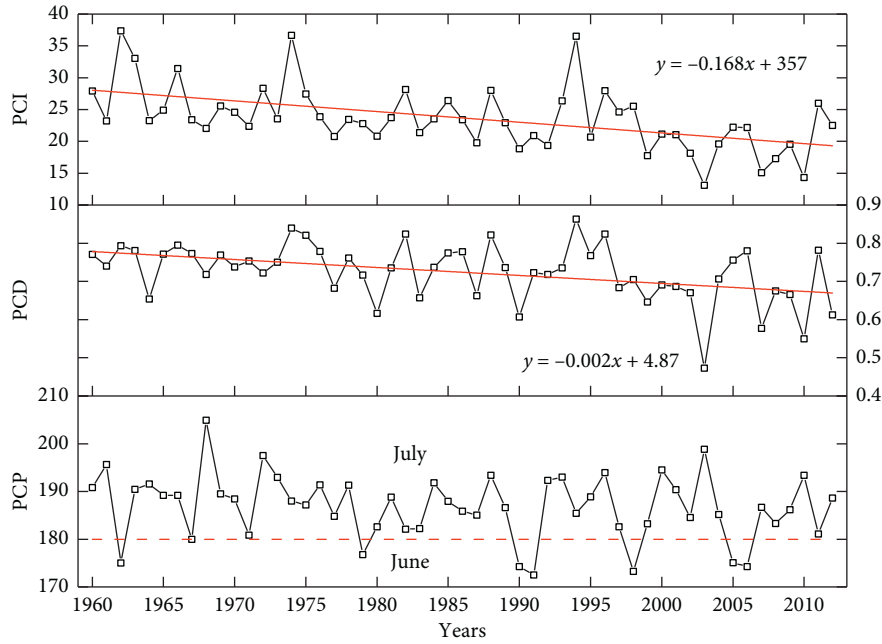


FIGURE 5: Time series of PCI, PCD, and PCP over the period of 1960–2012. The red solid line indicates the linear regression trend. The red dashed line means the boundary between the months June and July for the PCP. If the PCP is lower than 180, the maximum monthly precipitation appears in June. If the PCP ranges from 180 to 210, the maximum value appears in July.

TABLE 4: Results of change point analysis for different series based on the Pettitt test.

	Entire series (mm)	Change point	<i>p</i>	Prechange mean (mm)	Postchange mean (mm)	Ratio of changes ¹
Jan	2.2	2001	0.487	2.3	1.8	-0.23
Feb	4.6	1986	0.166	5.3	3.9	-0.30
Mar	9.0	1991	0.612	9.4	8.4	-0.11
Apr	20.5	1997	0.327	19	24.4	0.26
May	33.6	1976	0.042**	22.9	38.6	0.47
Jun	77.2	1975	0.295	62.2	83.7	0.28
Jul	180.7	1998	0.060*	195.7	139.2	-0.31
Aug	142.2	1996	0.024**	161.8	96.7	-0.46
Sep	50.6	1985	0.540	44.7	56.3	0.23
Oct	22.2	1995	0.424	20	26.9	0.31
Nov	7.8	1967	1.121	3.2	8.6	0.69
Dec	2.2	1973	0.124	0.8	2.7	0.86
Spring	63.1	1976	0.147	49.8	69.4	0.31
Summer	400.1	1996	0.043**	430.4	330.1	-0.25
Autumn	80.7	1988	0.690	73	89.9	0.21
Winter	8.9	1996	1.380	8.5	9.8	0.15
Annual	553.0	1996	0.398	573.5	505.6	-0.12

Note. ¹The ratio of change is equal to the differences of mean precipitation between prior series and posterior series dividing the mean precipitation at the entire series. *Significant abrupt change at a level of $\alpha=0.10$; **significant abrupt change at level of $\alpha=0.05$.

regression were almost similar to the precipitation trends found by the M-K test and Sen’s slope estimator. Both positive and negative trends were identified by the statistical tests in annual precipitation data. Only one station (ZT) showed significantly decreasing trend at a level of $\alpha=0.05$. All the other stations showed no significant decreasing or increasing trend at the 95% confidence level. For these stations with insignificant trend, seven stations showed a slight increasing trend and twenty-two stations showed a decreasing trend. The declining trend of most stations was similar to the change of regional annual precipitation over

Beijing. From the distribution of the annual precipitation trend, we can see that the highest value of precipitation decline mostly occurred in the southwest part of Beijing with a rate of more than 2mm/a. From the linear trend (Figure 6(f)), only three stations (NGZ, SZ, and ZJF) have slight increasing trend (less than 1 mm/a) and the other stations have decreasing trend with an average of 12.2 mm/10a. The WJY, XYL, and TYK stations have a clear decreasing trend with a value larger than 20 mm/10a.

Many studies have reported that changes in precipitation pattern are associated with elevation changes, although the

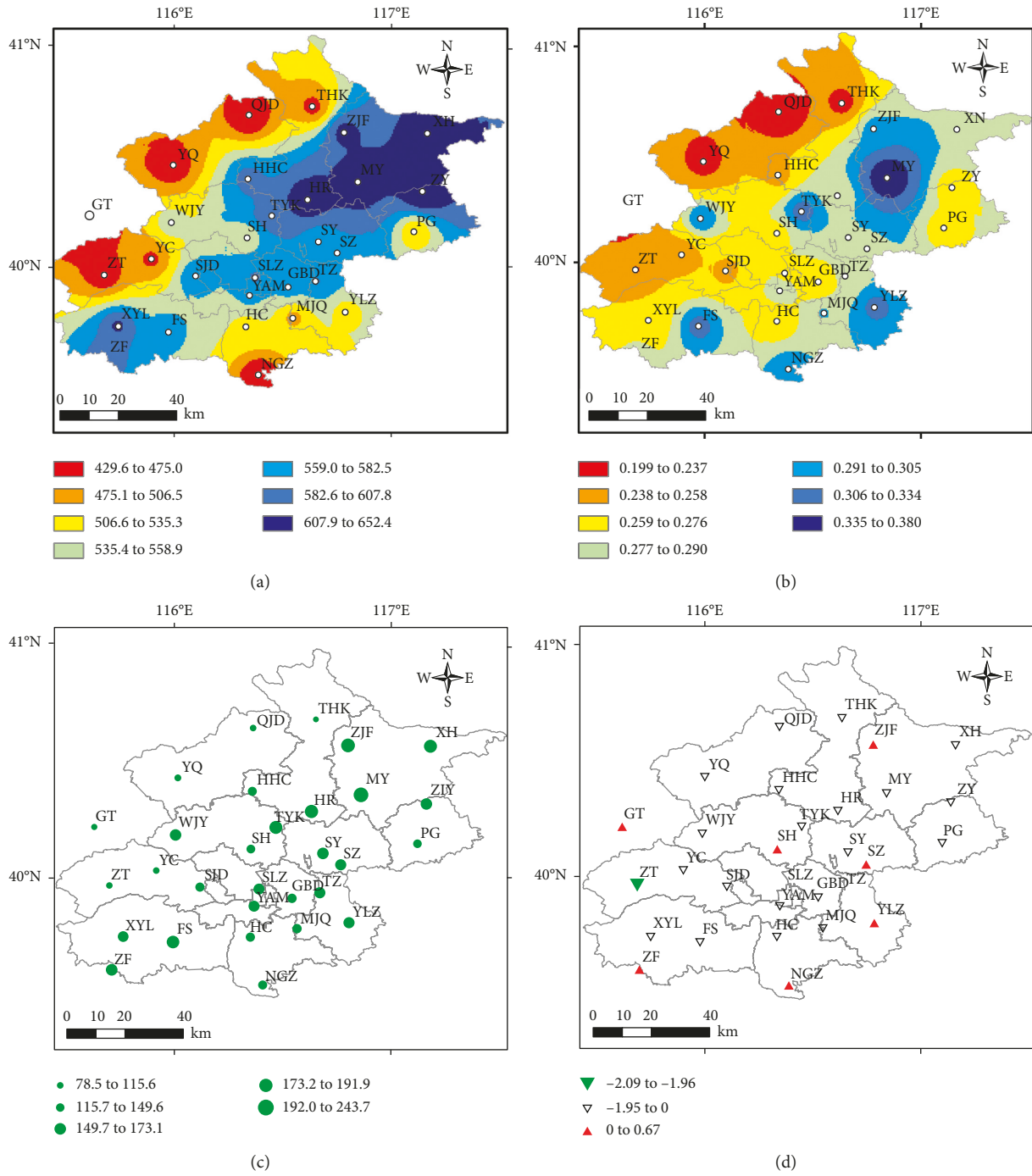


FIGURE 6: Continued.

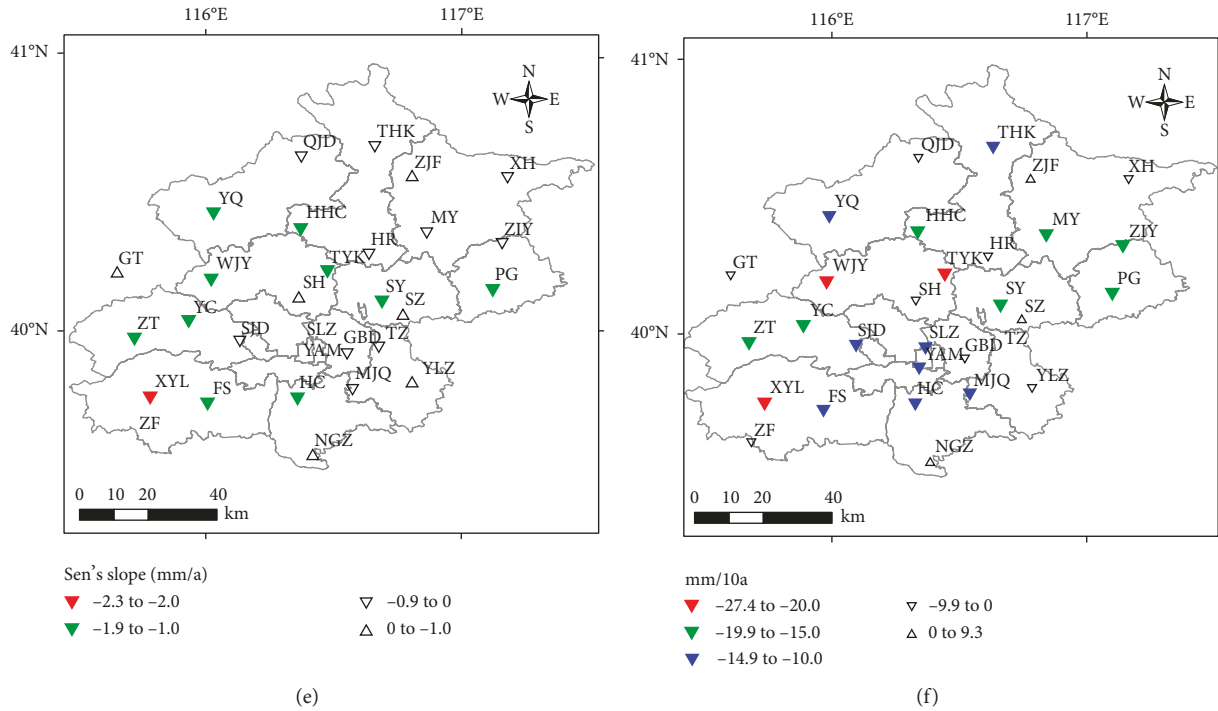


FIGURE 6: The spatial distribution of mean precipitation and their statistical characteristics and trends in Beijing during 1960–2012: (a) the annual mean precipitation, (b) the coefficient of variation, (c) the standard deviation, (d) the M-K test, (e) Sen's slope, and (f) the linear trend.

relationships can vary regionally. To investigate the relationship between the precipitation characteristics and elevation, we calculated the correlations between the 53-year (1960–2012) average precipitation amount and all station elevations, as shown in Figure 7. The results show that standard deviation and coefficient of variation are negatively and significantly correlated with elevation, with Pearson correlation coefficients higher than 0.5 ($p < 0.01$). A weak but significant negative relationship is also observed for precipitation amount with correlation of 0.45 ($p < 0.05$). These strong correlations between the precipitation and elevation indicate that local elevation has important impacts on the magnitude of precipitation in Beijing. Box plots show that the largest mean values of precipitation and standard deviation appear at 100~200 m, while the highest value of coefficient of variation occur at 0~100 m. Overall, therefore, the precipitation decreases with altitude, and higher precipitation events occur at lower altitudes in this area with higher coefficient of variation and standard deviation.

Regarding the analysis of the change points in the mean, the results for all the 30 rain gauges are summarized in Table 5 using the Pettitt test. As shown, change from positive to negative direction was detected for the 25 stations with a ratio of change from 7% to 22%. Only two stations (PG and ZT) presented significant change point at a level of $\alpha = 0.10$, which occurred in the years 1997 and 1996, respectively. We found most of change points (21 stations) detected based on Pettitt test occurred in the end of 1990s (1996–1998) without any statistical significant levels. The average change was about 16% of the annual mean precipitation in the entire

series with a negative change for all of these 21 stations. As discussed in Section 3.1, Beijing suffered from the continuous drought with continued 12 years since the end of 1990s, which is consistent with the results of change point analysis.

3.3. Changes of Different Precipitation Grades in the Flood Season. According to the results of PCI (Figure 5), we know that the uneven distribution of precipitation in Beijing is evident. We can see that the most of precipitation amount in Beijing happened in the flood season (June–July–August–September). In this study, the changes of precipitation grades were discussed based on the daily precipitation data in the flood season. Summary statistics of precipitation frequency, amount, and intensity for different grades of precipitation are presented in Table 6. The mean number of precipitation frequency is largest for small precipitation, with a value of 27, accounting for 67.8% of the total rainy days. The lowest number of days belongs to the heavy precipitation category, at about 1–2 days every year during the flood season. The characteristics of precipitation amount differ from that of the frequency for different grades of precipitation. The lowest value of precipitation amount belongs to the small precipitation, although its frequency is the highest. For the other three categories, their precipitation amounts are almost equivalent, at about 120 mm per year. However, the standard deviation of precipitation amount for heavy precipitation is largest. This explains the interannual variation for heavy precipitation is relatively larger than other categories. To a certain extent, the high variation of

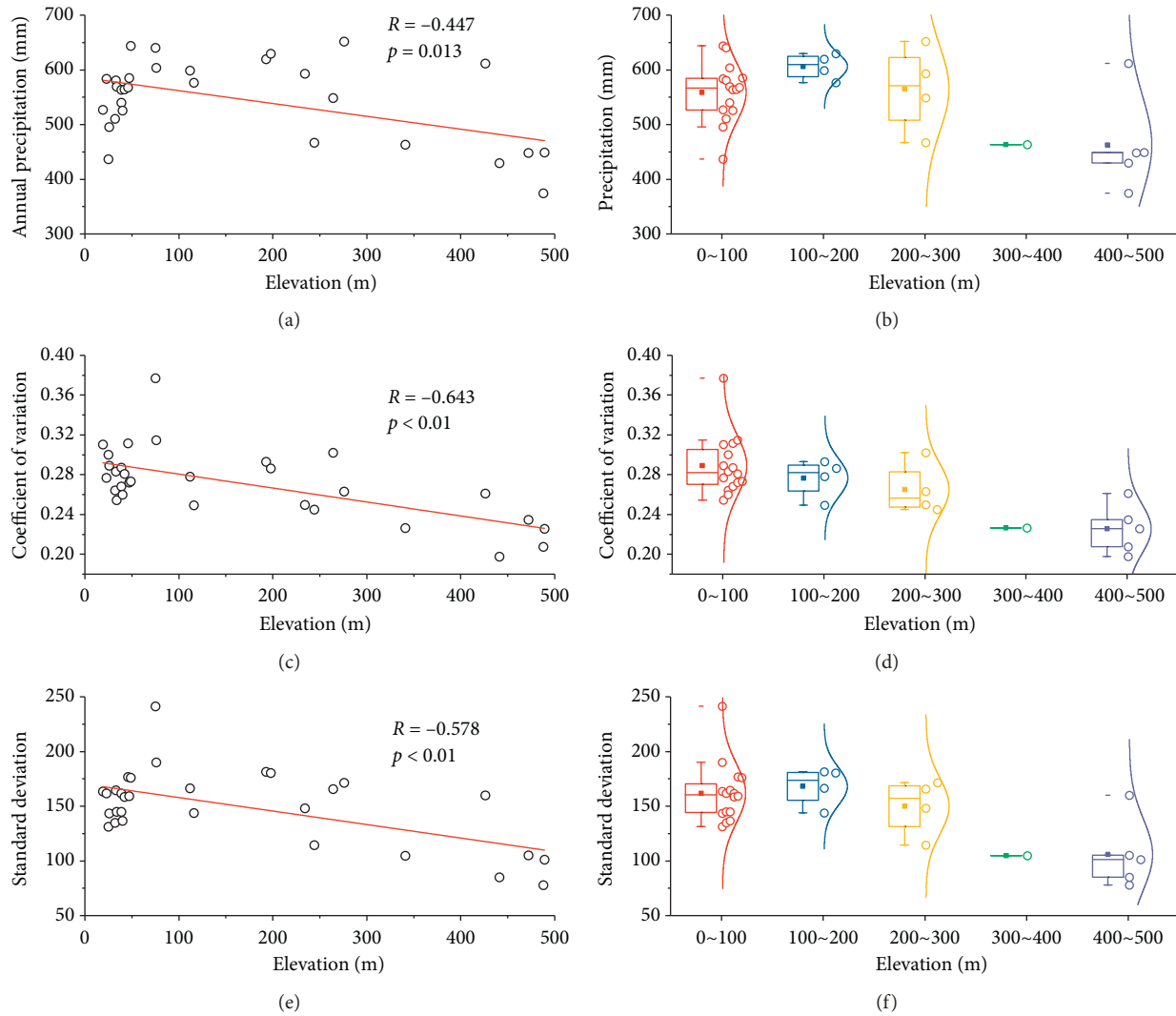


FIGURE 7: Scatter and box-plots in the correlations between precipitation characteristics and elevation. Solid red line is the linear trend. R signifies the Pearson correlation coefficient for each relationship and p indicates the statistical significance. The solid square means the mean value during the different elevation bands.

heavy precipitation might increase the degree of uncertainty of precipitation amount. A relatively obvious decline in precipitation amount for the heavy precipitation is shown based on the linear regression coefficient. This change might cause the change in precipitation amount in the flood season over Beijing.

Figure 8 also shows the ranges of precipitation frequency and amount for different grades. The frequency ranges from 16.9 to 39.4, 3.9 to 10.7, 1.7 to 6.1, and 0.2 to 3.1 for the small, medium, large, and heavy precipitations, respectively. The amount is ranging from 45 to 118.6 mm, 60 to 172.7 mm, 54.7 to 212.7 mm, and 16.7 to 314.2 mm for the different grades, respectively. In this work, PI and PC are used to further analyze the changes in different grades of precipitation, as also shown in Figure 8. Overall, the largest value of PI belongs to the small precipitation, accounting for 67% (54–77%) of all the rainy days. The mean values of PI for large and heavy precipitations are both smaller than 10% (9% and 4%). However, the value of PC for heavy

precipitation is larger than that of small precipitation. The largest value of PC is the medium precipitation, ranging from 18% to 40% with a mean of 29%. And the second belongs to the large precipitation, ranging from 18% to 37% with a mean of 27%. Additionally, the broad bound of PC (5–45%) for the heavy precipitation explains the relatively larger variation and higher degree of uncertainty. The detailed information about the PI and PC for 30 stations is shown in Figure S1.

In order to further discuss the spatial patterns of precipitation frequency and amount for the different grades, Figure 9 shows the spatial interpolation results of both indices for different grades. Overall, there are visible differences among the spatial patterns for the different grades of precipitation. For example, the frequency is increasing from east to west for the small precipitation, but it is increasing from south to north for the medium precipitation. From the perspective of precipitation amount, there are similar distribution patterns for the small and medium

TABLE 5: Results of change-point detection for different stations based on the Pettitt test.

Stations	Entire series	Change point	p	Prior series	Posterior series	Ratio of change ¹
FS	568.6	1996	0.229	599.0	496.4	-0.17
GBD	570.2	1998	0.494	591.5	509.3	-0.13
GT	374.4	1993	1.553	369.6	383.8	0.03
HR	641.7	1998	0.190	678.4	549.8	-0.19
HC	526.0	1998	0.773	546.3	467.9	-0.14
HHC	593.7	1998	0.465	617.9	524.6	-0.14
MJQ	496.8	1998	0.373	520.9	426.6	-0.17
MY	641.1	1998	0.672	675.1	543.9	-0.19
NGZ	437.1	2006	0.604	422.6	550.2	0.26
PG	511.3	1997	0.060*	541.9	431.7	-0.20
QJD	429.7	1992	0.571	440.1	404.8	-0.07
SJD	577.1	1996	0.921	597.6	527.7	-0.11
SH	539.1	1972	0.841	498.6	553.2	0.09
SY	564.3	1998	0.502	598.4	466.9	-0.21
SLZ	586.0	1998	0.344	612.0	511.6	-0.16
SZ	580.8	1998	0.773	602.4	522.1	-0.13
THK	464.0	1998	0.295	484.6	404.9	-0.15
TYK	604.6	1998	0.130	642.1	497.3	-0.22
TZ	584.1	1998	0.487	611.0	507.1	-0.16
WJY	550.0	1979	0.338	622.1	504.1	-0.20
XYL	612.0	1996	0.183	643.8	537.9	-0.16
XH	628.9	1975	1.046	573.6	654.2	0.12
YQ	449.0	1973	0.672	492.4	433.2	-0.12
YC	467.4	1979	0.213	513.8	438.8	-0.14
YAM	565.3	1998	0.285	591.4	490.7	-0.16
YLZ	527.3	1998	0.587	547.6	469.2	-0.14
ZT	448.6	1996	0.094*	471.8	393.8	-0.15
ZF	598.2	1996	1.282	614.0	564.6	-0.08
ZJF	618.5	1975	0.451	561.5	644.7	0.12
ZLY	652.4	1998	0.176	689.4	546.9	-0.20

Note. ¹The ratio of change is equal to the differences of mean precipitation between prior series and posterior series dividing the mean precipitation at the entire series. *Significant abrupt change at a level of $\alpha = 0.10$.

TABLE 6: Summary statistics for the precipitation frequency, amount, and intensity for the different grades.

	Frequency (days)			Amount (mm)			Intensity (mm/day)		
	Mean	SD	RC (days/10a)	Mean	SD	RC (mm/10a)	Mean	SD	RC (mm/(day-10a))
Small	27.0	3.37	-0.103	80.5	8.50	-0.644	3.0	0.33	-0.033
Medium	7.7	0.76	0.051	122.4	12.03	0.36	15.9	0.23	-0.071
Large	3.6	0.60	-0.148	124.4	21.49	-5.033	34.3	0.55	-0.009
Heavy	1.5	0.50	-0.13	121.7	42.61	-10.506	79.6	5.19	-1.255

Note. SD, standard deviation; RC, regression coefficient.

precipitation. The precipitation amount of small precipitation ranges from 65.1 to 95.9 mm, which declines from northwest to southeast. However, it declines from north to south for the medium precipitation, ranging from 95.9 to 148.9 mm. Additionally, the spatial distribution of precipitation frequency and amount for the large and heavy precipitation are almost similar to the distribution of the annual precipitation (Figure 6(a)). The relationship between the precipitation frequency and amount for different precipitation grades and elevation was also discussed in this work, as shown in Figure 10. For small and medium precipitation events, both frequency and amount have positive correlations with elevation, with no significance for frequency in small precipitation and amount in medium precipitation events. While for large and heavy precipitation

events, both have negative and significant correlations with elevation at a confidence level of 0.01. In conclusion, to a certain extent, the spatial distributions of precipitation frequency and amount are affected by the terrain. The large and heavy precipitations frequently occur in the plain areas, especially for the piedmont plain areas. But, in contrast, the precipitation of the mountain areas is dominated by the small and medium precipitations both in frequency and amount.

3.4. Differences in Changes of Precipitation in Four Subregions.

The variations of annual precipitation series for different subregions (i.e., plain area, mountain area, urban area, and suburban area) are shown in Figure 11, with the statistical

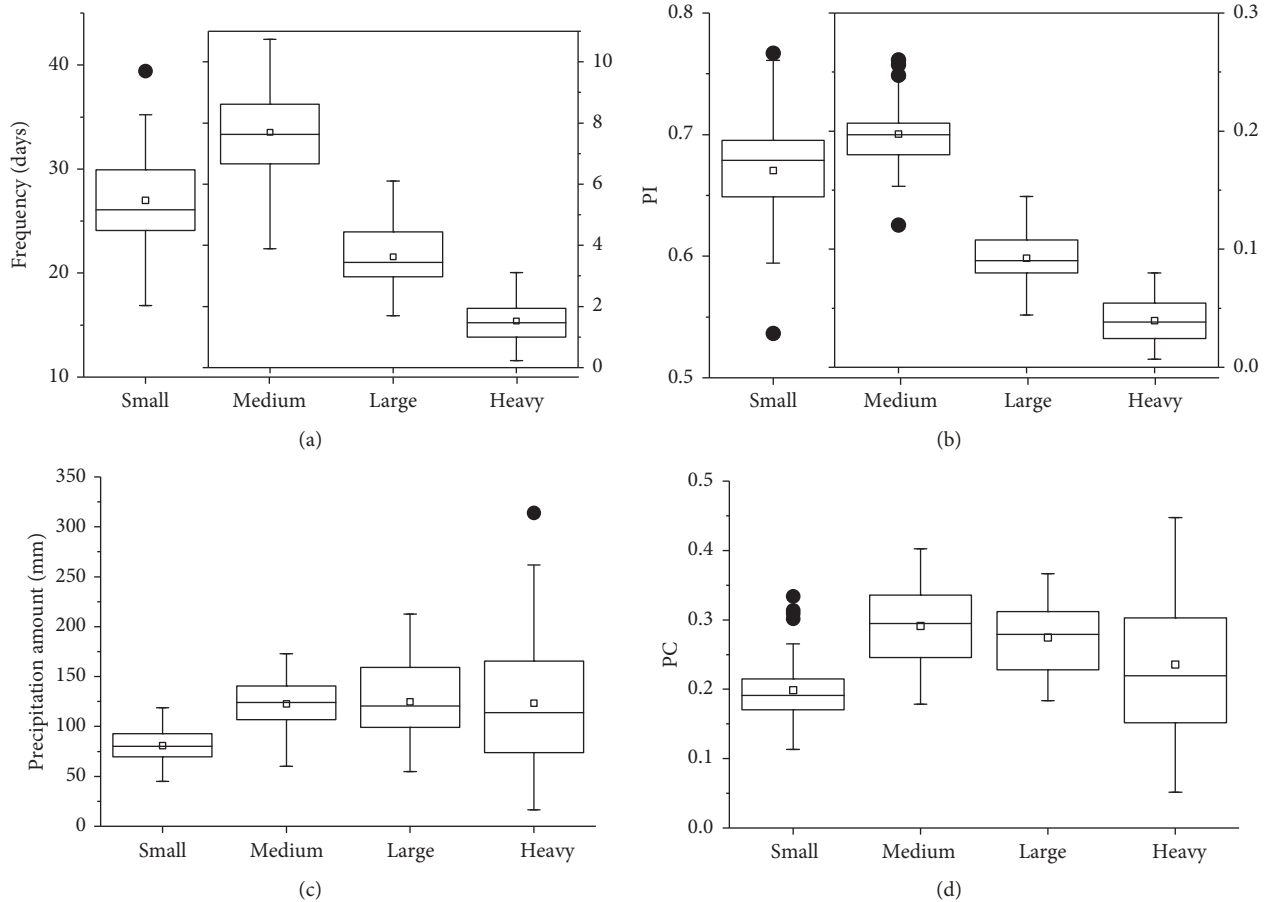


FIGURE 8: Box-plots of precipitation frequency (a), precipitation amount (b), precipitation incidence (c), and precipitation contribution (d) for different grades of precipitation over Beijing during 1960–2012. The boxes indicate the 25th, 50th, and 75th percentiles and the whiskers indicate the values with maximum 1.5 interquartile ranges. The hollow square indicates the mean value. The solid circle means the outlier.

results given in Table 7. As a whole, we found that the average precipitation amount in the area of the Beijing Plain (urban area) was greater than that in the mountainous (suburban) areas. As seen in Figure 11, the precipitation showed slight decreasing trends at the rate of 6.4 and 9.9 mm/decade for the plain and mountain areas (Figure 11(a)), 4 and 4.9 mm/decade for the urban and suburban areas (Figure 11(c)) during 1960–2012, respectively. However, as shown in Figure S2, from the standpoint of the changes in built-up areas, the urban expansion has experienced three stages in Beijing during the research period: the first stage is the slowest urban expansion before 1980, the second is the rapid expansion stage from 1980 to 2000, and the third is the fastest urban growing period during the first decade of the 21st century [3]. Therefore, the changes in precipitation during the three stages for these areas are also discussed. During 1960–1979, the difference of the precipitation amount between areas in the plain and the mountains was about 24.2 mm, which accounts for 4.15% of the total precipitation in the plain areas, while the difference between urban areas and suburb areas was 32.9 mm, accounting for 5.51% of the total precipitation in the urban areas. During 1980–1999, the

difference has expanded to 32.6 mm (accounting for 5.72% of the total precipitation in the plain areas) between the areas in the plain and mountains and 45.2 mm (accounting for 7.66% of the total precipitation in the urban areas) between the urban areas surrounding suburb areas. It is clear that the average precipitation decreased both in the urban and suburb areas through these two periods, while the drying was larger in the suburb areas, which caused the higher differences in precipitation between the urban and surrounding suburb areas. With rapid development of urbanization, the height and density of buildings are both increasing, and the rainfall under a weather system in urban areas would stay longer than that in open suburb areas [56]; thus, the total precipitation increased. Additionally, in the process of urbanization, population density increases in cities, releasing more heat into the atmosphere and changing the imperviousness of underlying areas. All these factors lead to an urban heat island effect, leading to precipitation variations in urban areas. However, during 2000–2012, the precipitation amount in the above four areas has declined by 49.8–67.9 mm compared with the last period due to the long-term drought (1999–2010) in the north China, accounting for 8.5–11.6% of the average annual precipitation (584.7 mm)

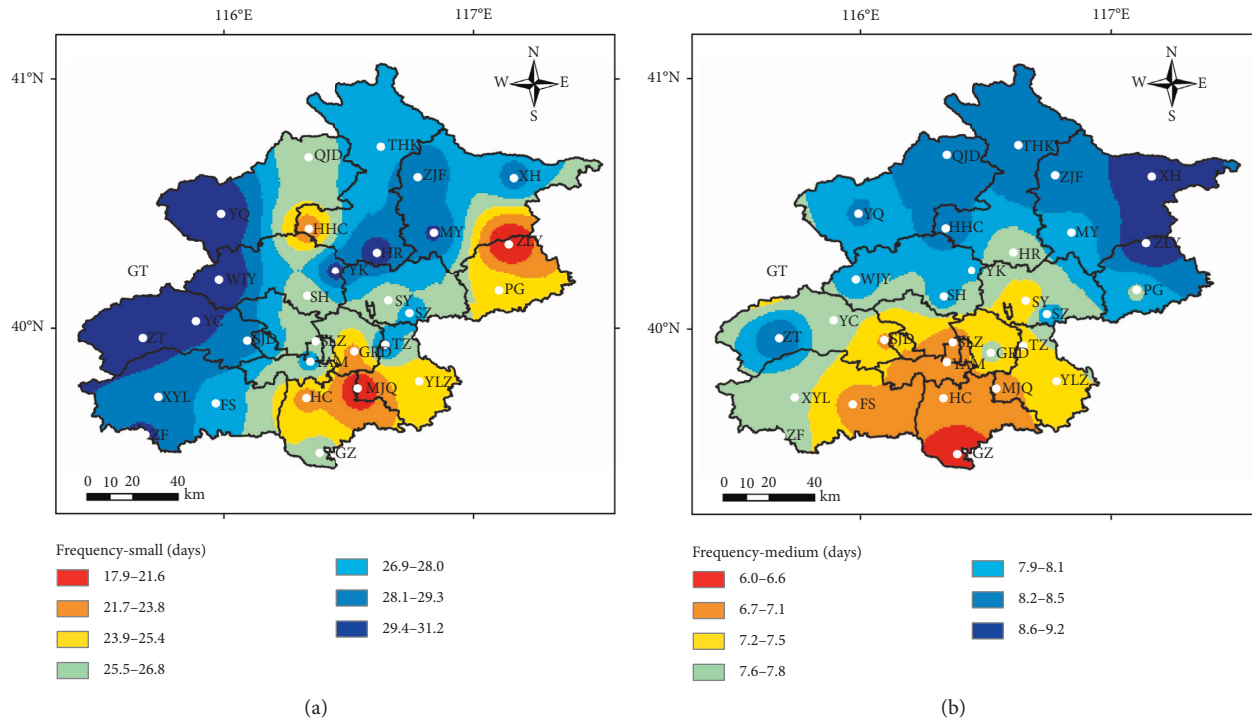


FIGURE 9: Continued.

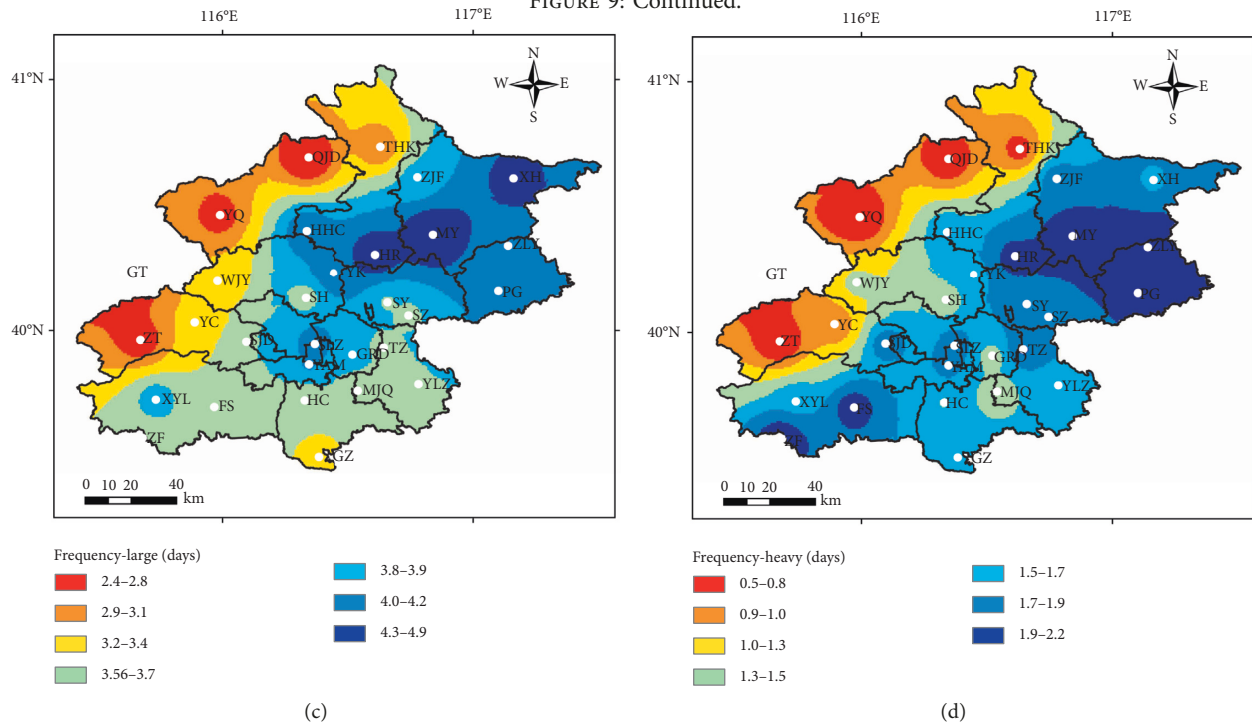


FIGURE 9: Continued.

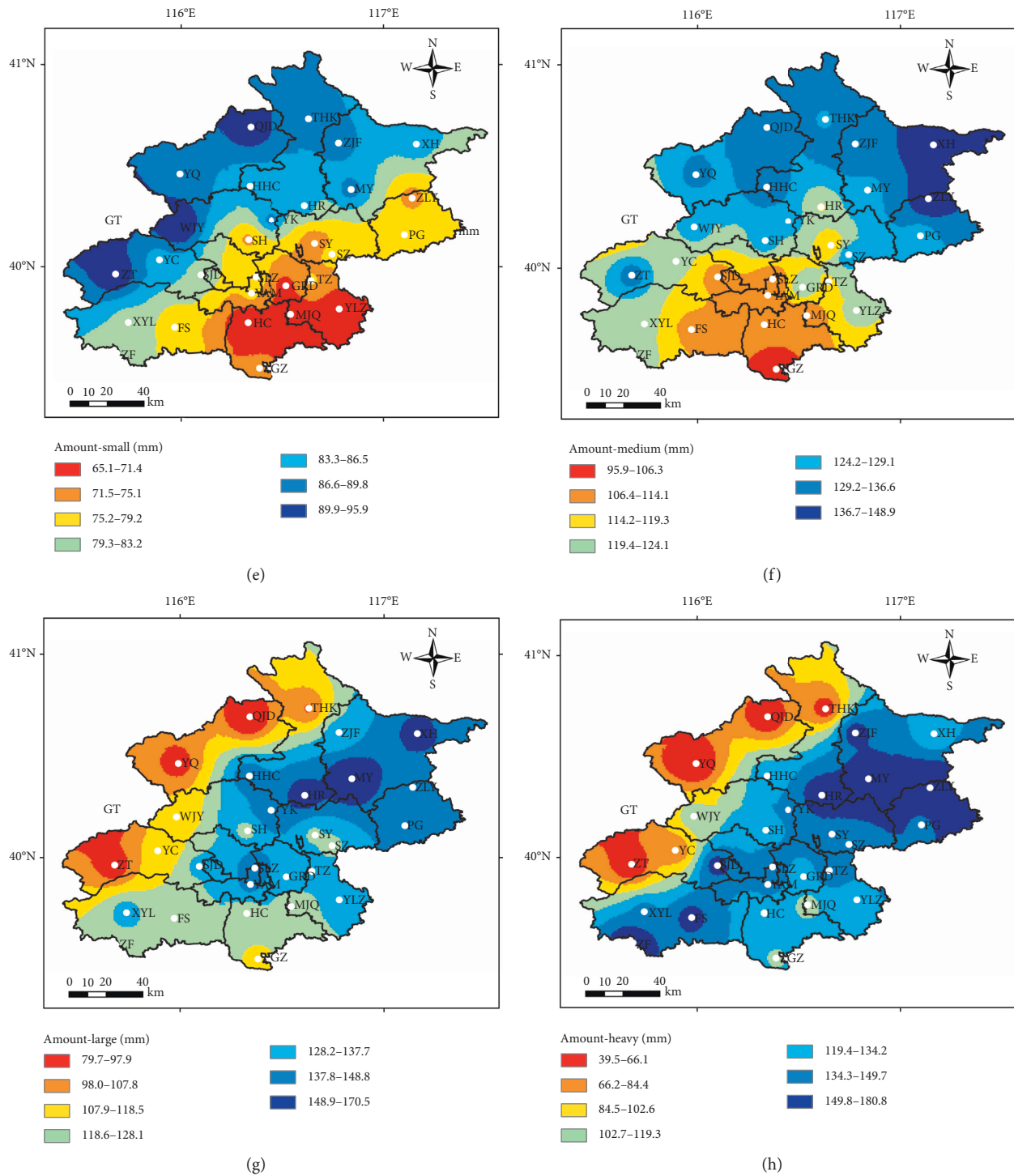


FIGURE 9: Spatial distribution of precipitation frequency and amount for the different grades during 1960–2012. (a, e) Small precipitation. (b, f) Medium precipitation. (c, g) Large precipitation. (d, h) Heavy precipitation.

over Beijing. During this period, Table 7 showed that the difference dropped to 17.7 mm (accounting for 3.51% of the total precipitation in the plain areas) between the plain and mountains and 31.0 mm (accounting for 5.94% of the total precipitation in the urban areas) in the urban and surrounding suburb areas. Moreover, the difference in precipitation between the plain and mountain areas had a

slightly increasing trend at a rate of 3.49 mm/decade during the period of 1960–2012 (Figure 12(a)). The increasing rate for the difference between the plain and mountain areas was larger than that for the difference between urban and suburban areas (0.87 mm/decade) (Figure 12(b)). However, the results of M-K test and Sen’s slope estimate showed that there was a nonsignificant decreasing trend for the

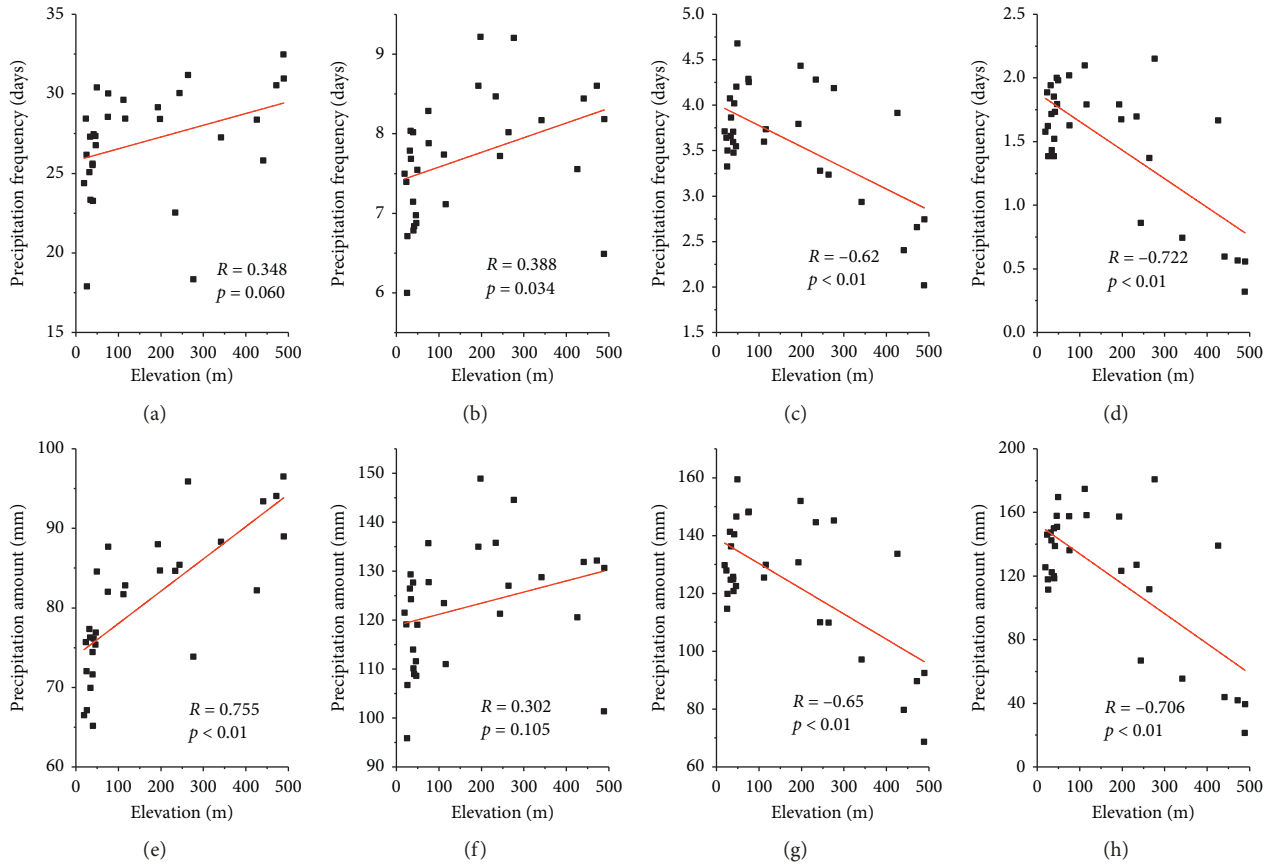


FIGURE 10: Spatial distribution of precipitation frequency and amount for the different grades during 1960–2012. (a, e) Small precipitation. (b, f) Medium precipitation. (c, g) Large precipitation. (d, h) Heavy precipitation.

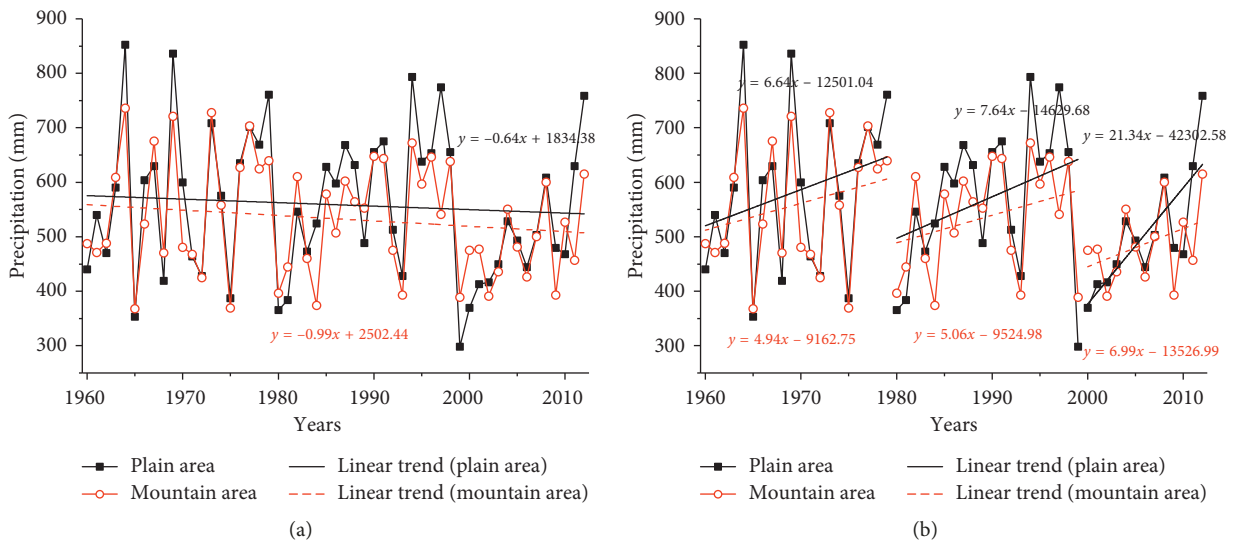


FIGURE 11: Continued.

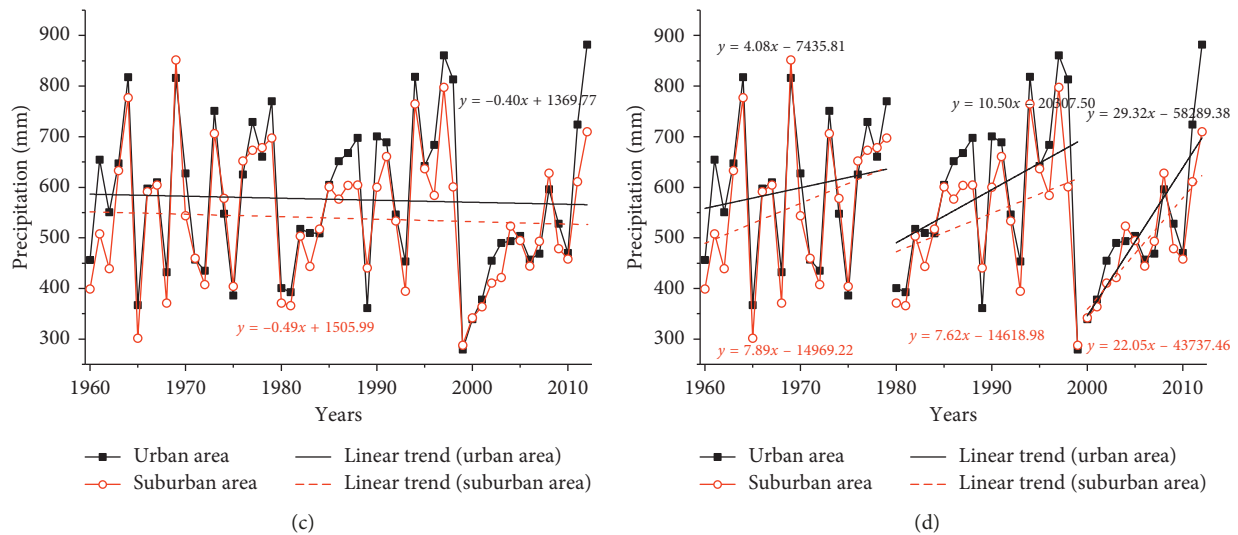


FIGURE 11: Time series of annual mean precipitation in the plain and mountain areas (top panel) and the urban and suburb areas (bottom panel). The linear trend analyses are discussed based on the different periods: one (left panel) is based on the whole period (1960–2012) and another one (right panel) is based on the three subperiods (1960–1979, 1980–2000, and 2001–2012) considering the different urban expansion stages.

TABLE 7: Comparison of mean precipitation in the different subregions and periods.

	Plain area	Mountainous area	Percent of differences (%) ¹	Urban area	Suburb area	Percent of differences (%) ¹
1960–1979	583.2	559.0	4.15	597.0	564.1	5.51
1980–1999	569.6	537.0	5.72	589.9	544.7	7.66
2000–2012	504.8	487.1	3.51	522.0	491.0	5.94
1960–2012	558.8	533.0	4.62	575.9	538.9	6.42

Note. The percent of differences = the differences in precipitation between the plain (urban) and mountainous (suburb) areas divided by the total amount of precipitation in the plain (urban) areas.

differences in precipitation between the urban and suburban areas.

4. Conclusions

In this study, a comprehensive investigation was performed on the precipitation changes across Beijing based on the monthly, seasonal, and annual mean precipitation from 30 rain gauges from 1960 to 2012. Many time series analysis methods, evaluating indicators, and tools were used to assess the variations of precipitation structure. Based on our analysis, main findings are summarized as follows.

The annual mean precipitation has a clear decreasing trend at a rate of 11.6 mm/10a during the period of 1960–2012. Seasonally, a significant decrease in precipitation occurred in summer (21.1 mm/10a). In contrast, the precipitation in spring shows a significant increasing trend with a rate of 4.7 mm/10a. There are nonsignificant trends in autumn and winter. However, this increase in spring is unable to offset the remarkable decrease in summer, which is a dominant driver for the decline in annual precipitation. Similarly, the monthly series of precipitation in January, February, July, and August show a significant decreasing trend while that in May has a statistically significant increase.

These changes, to some extent, lead to the significant change in spring and summer.

Overall, there is no change in a strongly uneven spatiotemporal distribution in precipitation within the Beijing metropolis. Although the PCI and PCD both have a decreasing trend, they are both in a relatively high level, which is an inherent characteristic for the East Asian Monsoon areas. These declines may be dominantly caused by the significant decrease in precipitation in summer and the increases in spring and autumn. Simultaneously, the precipitation roughly decreases from east to west due to the orographic effects, with the highest rain occurring at the Miyun and Huairou reservoirs in the northeast and the lowest in the northwestern mountain areas. In addition, the effects of urban development on precipitation become more and more obvious.

The spatiotemporal changes for the four precipitation grades (small, median, large, and heavy) are different. In general, the frequency for the small precipitation is the largest, followed by the median and large precipitations, and that for the heavy precipitation is the lowest. On average, the amount for the small precipitation is the lowest and the other three grades are almost equivalent. The spatial distribution for different grades are affected by the terrain; the

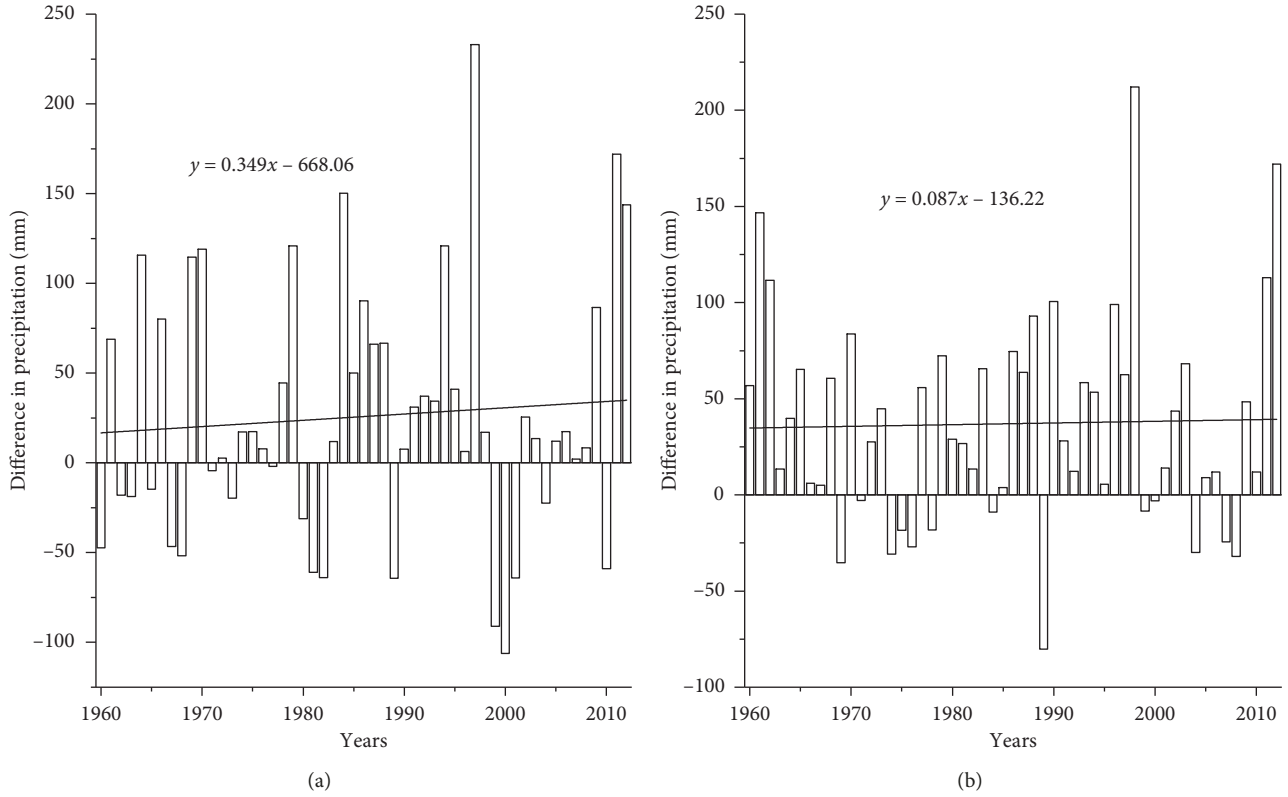


FIGURE 12: Differences in precipitation and their linear trends: (a) between the plain and mountain areas, (b) between the urban and suburban areas.

large and heavy precipitation frequently occur in the plain areas, while the precipitation in the mountain areas is dominated by the small and medium precipitations.

In the current context of global climate change and rapid urban development in Beijing, adaptations for avoiding or minimising their impacts on water resources require analysis of the change in precipitation patterns on a fine spatio-temporal scale. The adverse natural conditions and the rapid urban development in Beijing lead to the high risk in the urban water resources management. For example, Beijing suffers the problems both in water deficit and urban flood and waterlogging in recent years. To some extent, these problems are probably caused by the change in precipitation pattern. Therefore, the future work should be paid attention to the relationship between the change in precipitation and the urban water resources safety, in order to obtain deep understanding and knowledge.

Appendix

Mann-Kendall trend test and Sen's slope estimate method were widely used to detect trends in hydrological and meteorological time series. The detailed information was introduced as follows:

In the M-K trend test, the null hypothesis (H_0) is that the data in a time series are independent and identically distributed random variables and the hypothesis (H_1) is that there is a trend in the series. Statistical parameter (S_0) is defined as

$$S_0 = \sum_{k=1}^{n-1} \sum_{j=k+1}^n \text{sgn}(x_j - x_k), \quad (\text{A.1})$$

where n is the length of the series, $k = 1, 2, \dots, n-1, j = 2, 3, \dots, n$, and

$$\text{sgn}(x_j - x_k) = \begin{cases} 1, & (x_j - x_k) > 0, \\ 0, & (x_j - x_k) = 0, \\ -1, & (x_j - x_k) < 0. \end{cases} \quad (\text{A.2})$$

It has been proven that when $n \geq 8$, S_0 follows approximately the normal distribution with 0 mean and the variance as

$$\text{Var}(S_0) = \frac{[n(n-1)(2n+5)]}{18}. \quad (\text{A.3})$$

Standardized statistic Z can be Calculated as

$$Z = \begin{cases} \frac{S_0 - 1}{\sqrt{\text{Var}(S_0)}}, & S_0 > 0, \\ 0, & S_0 = 0, \\ \frac{S_0 + 1}{\sqrt{\text{Var}(S_0)}}, & S_0 < 0. \end{cases} \quad (\text{A.4})$$

Negative Z value denotes downward trend and positive Z value shows upward trend. The trend is significant at the 95% confidence level $|Z| > 1.96$ and vice versa.

In Sen's slope estimator method, the slope of trend in the sample of N pairs of data is calculated by

$$Q_i = \frac{x_j - x_k}{j - k}, \quad \text{for } i = 1, 2, \dots, N, \quad (\text{A.5})$$

where x_j and x_k are the data values at times j and k ($j > k$), respectively. If there is only one datum in each time period, then $N = n(n-1)/2$, where n is the number of time periods. If there are multiple observations in one or more time periods, then $N < n(n-1)/2$, where n is the total number of observations.

The N values of Q_i are ranked from smallest to largest and the median of slope is computed as

$$Q_{\text{med}} = \begin{cases} Q_{[(N+1)/2]}, & \text{if } N \text{ is odd,} \\ \frac{Q_{[N/2]} + Q_{[(N+2)/2]}}{2}, & \text{if } N \text{ is even.} \end{cases} \quad (\text{A.6})$$

The Q_{med} sign reflects data trend reflection, while its value indicates the steepness of the trend. To determine whether the median slope is statistically different from zero, one should obtain the confidence interval of Q_{med} at specific probability. The confidence interval about the time slope can be computed as follows:

$$C_\alpha = Z_{1-\alpha/2} \sqrt{\text{Var}(S_0)}, \quad (\text{A.7})$$

where $Z_{1-\alpha/2}$ is obtained from the standard normal distribution table. In this study, the confidence interval was computed at a significant level of $\alpha = 0.05$. Then, $M_1 = (N - C_\alpha)/2$ and $M_2 = (N + C_\alpha)/2$ are computed. The lower and upper limits of the confidence interval, Q_{min} and Q_{max} , are the M_1^{th} largest and the $(M_2 + 1)^{\text{th}}$ largest of the N ordered slope estimates. The slope Q_{med} is statistically different from zero if the two limits have similar sign.

Data Availability

Rainfall data supporting this article are available from the Hydrological Data of Haihe River Basin (in Chinese) and the Annual Hydrological Report of China (Volume III), released by Ministry of Water Resources of China. For further information or right to access to the material used in this paper, readers can also contact the Beijing Hydrological Stations of the Beijing Water Authority (<http://www.bjwater.gov.cn>). For the other data used in this article, readers can contact the corresponding author X. Song.

Conflicts of Interest

The authors declare that there are no conflicts of interest regarding the publication of this paper.

Acknowledgments

This work was supported by the Fundamental Research Funds for the Central Universities (2015XKMS034), the

National Natural Science Foundation of China (51609242), the National Key Research and Development Program (2017YFC1502701), the China Postdoctoral Science Foundation (2018M632333), the Open Research Fund Program of State Key Laboratory of Water Resources and Hydropower Engineering Science (2015SWG02), and the Open Research Fund Program of State Key Laboratory of Hydrology-Water Resources and Hydraulic Engineering (2015490411). The authors would like to thank the Beijing Hydrologic Stations of Beijing Water Authority in China for providing all of the precipitation data.

Supplementary Materials

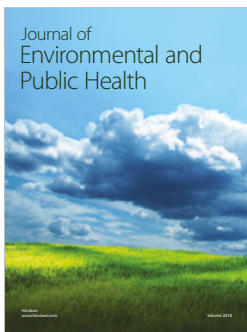
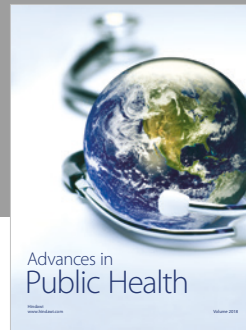
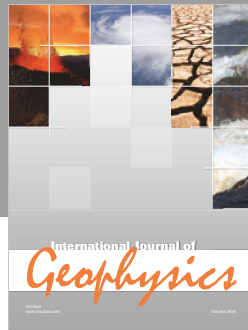
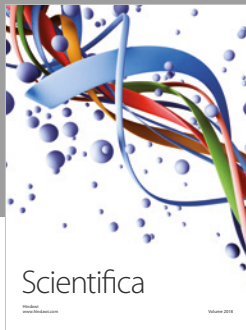
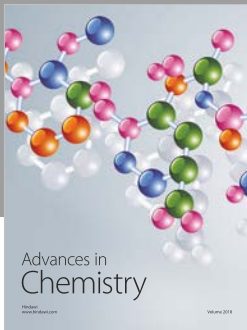
Figure S1: the incidence (PI) and contribute (PC) of different precipitation grades to the total frequency and amount for the 30 stations during 1960–2012. Figure S2: the urban built-up areas in Beijing during 1950–2012. (*Supplementary Materials*)

References

- [1] C. Chen and W. Huang, "Hydrological modeling of typhoon-induced extreme storm runoffs from Shihmen watershed to reservoir, Taiwan," *Natural Hazards*, vol. 67, no. 2, pp. 747–761, 2013.
- [2] H. Chang and W. T. Kwon, "Spatial variations of summer precipitation trends in South Korea, 1973–2005," *Environmental Research Letters*, vol. 2, no. 4, article 045012, 2007.
- [3] X. Song, J. Zhang, A. AghaKouchak et al., "Rapid urbanization and changes in spatiotemporal characteristics of precipitation in Beijing metropolitan area," *Journal of Geophysical Research: Atmospheres*, vol. 119, no. 19, pp. 11250–11271, 2014.
- [4] Y. Zhai, Y. Guo, J. Zhou, N. Guo, J. Wang, and Y. Teng, "The spatio-temporal variability of annual precipitation and its local impact factors during 1724–2010 in Beijing, China," *Hydrological Processes*, vol. 28, no. 4, pp. 2192–2201, 2014.
- [5] S. Dawadi and S. Ahmad, "Changing climatic conditions in the Colorado River Basin: implications for water resources management," *Journal of Hydrology*, vol. 430–431, pp. 127–141, 2012.
- [6] V. Kumar, S. K. Jain, and Y. Singh, "Analysis of long-term rainfall trends in India," *Hydrological Sciences Journal*, vol. 55, no. 4, pp. 484–496, 2010.
- [7] A. Kalra and S. Ahmad, "Evaluating changes and estimating seasonal precipitation for the Colorado River Basin using a stochastic nonparametric disaggregation technique," *Water Resources Research*, vol. 47, no. 5, article W05555, 2011.
- [8] S. Sagarika, A. Kalra, and S. Ahmad, "Evaluating the effect of persistence on long-term trends and analyzing step changes in streamflows of the continental United States," *Journal of Hydrology*, vol. 517, pp. 36–53, 2014.
- [9] J. Wang, J. Feng, Z. Yan, Y. Hu, and G. Jia, "Nested high-resolution modeling of the impact of urbanization on regional climate in three vast urban agglomerations in China," *Journal of Geophysical Research: Atmospheres*, vol. 117, no. D21, 2012.
- [10] J. Zhang, X. Song, G. Wang et al., "Development and challenges of urban hydrology in a changing environment: I. Hydrological response to urbanization," *Advances in Water Science*, vol. 25, no. 4, pp. 594–605, 2014, in Chinese with English abstract.

- [11] E. Kalnay and M. Cai, "Impact of urbanization and land-use change on climate," *Nature*, vol. 423, no. 6939, pp. 528–531, 2003.
- [12] D. Rosenfeld, "Suppression of rain and snow by urban and industrial air pollution," *Science*, vol. 287, no. 5459, pp. 1793–1796, 2000.
- [13] D. Rosenfeld, U. Lohmann, G. B. Raga et al., "Flood or drought: how do aerosols affect precipitation?," *Science*, vol. 321, no. 5894, pp. 1309–1313, 2008.
- [14] Y. Huang, S. Chen, Q. Cao et al., "Evaluation of version-7 TRMM multi-satellite precipitation analysis product during the Beijing extreme heavy rainfall events of 21 July 2012," *Water*, vol. 6, pp. 32–44, 2014.
- [15] M. Li, J. Xia, Z. Chen et al., "Variation analysis of precipitation during past 286 years in Beijing area, China, using non-parametric test and wavelet analysis," *Hydrological Processes*, vol. 27, pp. 2934–2943, 2013.
- [16] J.-Y. Han, J.-J. Baik, and H. Lee, "Urban impacts on precipitation," *Asia-Pacific Journal of Atmospheric Sciences*, vol. 50, no. 1, pp. 17–30, 2014.
- [17] Z. Han, Z. Yan, Z. Li, W. Liu, and Y. Wang, "Impact of urbanization on low-temperature precipitation in Beijing during 1960–2008," *Advances in Atmospheric Sciences*, vol. 31, no. 1, pp. 48–56, 2014.
- [18] J. Wang, R. Zhang, and Y. Wang, "Areal differences in diurnal variations in summer precipitation over Beijing metropolitan region," *Theoretical and Applied Climatology*, vol. 110, no. 3, pp. 395–408, 2012.
- [19] L. Yang, F. Tian, J. A. Smith, and H. Hu, "Urban signatures in the spatial clustering of summer heavy rainfall events over the Beijing metropolitan region," *Journal of Geophysical Research: Atmospheres*, vol. 119, no. 3, pp. 1203–1217, 2014.
- [20] N. Mölders and M. A. Olson, "Impact of urban effects on precipitation in high latitudes," *Journal of Hydrometeorology*, vol. 5, no. 3, pp. 409–429, 2004.
- [21] J. M. Shepherd, H. Pierce, and A. J. Negri, "Rainfall modification by major urban areas: observations from spaceborne rain radar on the TRMM satellite," *Journal of Applied Meteorology*, vol. 41, no. 7, pp. 689–701, 2002.
- [22] C. L. Zhang, F. Chen, S. G. Miao, Q. C. Li, X. A. Xia, and C. Y. Xuan, "Impacts of urban expansion and future green planting on summer precipitation in the Beijing metropolitan area," *Journal of Geophysical Research*, vol. 114, no. D2, p. D02116, 2009.
- [23] S. Dawadi and S. Ahmad, "Evaluating the impact of demand-side management on water resources under changing climatic conditions and increasing population," *Journal of Environmental Management*, vol. 114, pp. 261–275, 2013.
- [24] A. K. Venkatesan, S. Ahmad, W. Johnson, and J. R. Batista, "Systems dynamic model to forecast salinity load to the Colorado River due to urbanization within the Las Vegas Valley," *Science of the Total Environment*, vol. 409, no. 13, pp. 2616–2625, 2011.
- [25] X. Batista, Z. Wang, Y. Qi, and H. Guo, "Effect of urbanization on the winter precipitation distribution in Beijing area," *Science in China Series D: Earth Sciences*, vol. 52, no. 2, pp. 250–256, 2009.
- [26] S. Guo and J. Ma, "Impact of urbanization on precipitation in Beijing area," *Journal of the Meteorological Sciences*, vol. 31, no. 4, pp. 414–421, 2011, in Chinese with English abstract.
- [27] Z. Li, Z. Yan, K. Tu, and H. Wu, "Changes of precipitation and extremes and the possible effect of urbanization in the Beijing Metropolitan region during 1960–2012 based on homogenized observations," *Advances in Atmospheric Sciences*, vol. 32, no. 9, pp. 1173–1185, 2015.
- [28] S. Wu, F. Chen, M. A. LeMone, M. Tewari, Q. Li, and Y. Wang, "An observational and modeling study of characteristics of urban heat island and boundary layer structures in Beijing," *Journal of Applied Meteorology and Climatology*, vol. 48, no. 3, pp. 484–501, 2009.
- [29] S. Miao, F. Chen, and Q. Li, "Month-averaged impacts of urbanization on atmospheric boundary layer structure and precipitation in summer in Beijing area," *Chinese Journal of Geophysics*, vol. 53, no. 7, pp. 1580–1593, 2010, in Chinese with English abstract.
- [30] Z. Xu, L. Zhang, and B. Ruan, "Analysis on the spatio-temporal distribution of precipitation in the Beijing region," *Arid Land Geography*, vol. 29, no. 2, pp. 186–192, 2006, in Chinese with English abstract.
- [31] S. Yu, "Decadal rainfall variability over Beijing and the urban effect," *Advances in Nature Science*, vol. 17, no. 5, pp. 632–638, 2007, in Chinese with English abstract.
- [32] Y. Zhang, J. A. Smith, L. Luo, Z. Wang, and M. L. Baeck, "Urbanization and rainfall variability in the Beijing metropolitan region," *Journal of Hydrometeorology*, vol. 15, no. 6, pp. 2219–2235, 2014.
- [33] C. Zhang, C. Ji, Y. Kuo et al., "Numerical simulation of topography effects on the '00.7' severe rainfall in Beijing," *Progress in Natural Science*, vol. 15, no. 9, pp. 818–826, 2005.
- [34] J. Sun, H. Wang, L. Wang et al., "The role of urban boundary layer in local convective torrential rain happening in Beijing on 10 July 2004," *Chinese Journal of Atmospheric Sciences*, vol. 30, pp. 221–234, 2006, in Chinese with English abstract.
- [35] Q. Wu, H. Guo, B. Yang et al., "Effects of topography and urban heat circulation on a meso- β torrential rain in Beijing area," *Meteorology Monthly*, vol. 35, pp. 58–64, 2009, in Chinese with English abstract.
- [36] J. Sun and B. Yang, "Meso- β scale torrential rain affected by topography and the urban circulation," *Chinese Journal of Atmospheric Sciences*, vol. 32, pp. 1352–1364, 2008, in Chinese with English abstract.
- [37] A. Bárdossy and G. Pegram, "Infilling missing precipitation records - a comparison of a new copula-based method with other techniques," *Journal of Hydrology*, vol. 519, pp. 1162–1170, 2014.
- [38] R. S. V. Teegavarapu and V. Chandramouli, "Improved weighting methods, deterministic and stochastic data-driven models for estimation of missing precipitation records," *Journal of Hydrology*, vol. 312, no. 1–4, pp. 191–206, 2005.
- [39] X. M. Song, J. Y. Zhang, J. F. Liu et al., "Spatial-temporal variation characteristics of precipitation pattern in Beijing," *Journal of Hydraulic Engineering*, vol. 46, no. 5, pp. 525–535, 2015, in Chinese with English abstract.
- [40] J. E. Oliver, "Monthly precipitation distribution: a comparative index," *Professional Geographer*, vol. 32, no. 3, pp. 300–309, 1980.
- [41] L. J. Zhang and Y. F. Qian, "Annual distribution features of precipitation in China and their interannual variations," *Acta Meteorologica Sinica*, vol. 17, no. 2, pp. 146–163, 2003.
- [42] X. M. Li, F. Q. Jiang, L. H. Li et al., "Spatial and temporal variability of precipitation concentration index, concentration degree and concentration period in Xinjiang, China," *International Journal of Climatology*, vol. 31, pp. 1679–1693, 2011.
- [43] S. Fatichi, S. M. Barbosa, E. Caporali, and M. E. Silva, "Deterministic versus stochastic trends: detection and

- challenges,” *Journal of Geophysical Research*, vol. 114, no. D18, article D18121, 2009.
- [44] M. G. Silva, *Rank Correlation Methods*, Griffin, London, UK, 1975.
- [45] H. B. Mann, “Nonparametric tests against trend,” *Econometrica*, vol. 13, no. 3, pp. 245–259, 1945.
- [46] P. K. Sen, “Estimates of the regression coefficient based on Kendall’s Tau,” *Journal of the American Statistical Association*, vol. 63, no. 324, pp. 1379–1389, 1968.
- [47] Z. Bao, J. Zhang, G. Wang et al., “Attribution for decreasing streamflow of the Haihe River basin, northern China: climate variability or human activities?,” *Journal of Hydrology*, vol. 460-461, pp. 117–129, 2012.
- [48] W. Shi, X. Yu, W. Liao, Y. Wang, and B. Jia, “Spatial and temporal variability of daily precipitation concentration in the Lancang River basin, China,” *Journal of Hydrology*, vol. 495, pp. 197–207, 2013.
- [49] Q. Liu, Z. Yang, and B. Cui, “Spatial and temporal variability of annual precipitation during 1961-2006 in Yellow River basin, China,” *Journal of Hydrology*, vol. 361, no. 3-4, pp. 330–338, 2008.
- [50] Y. Dinpashoh, D. Jhajharia, A. Fakheri-Fard et al., “Trends in reference crop evapotranspiration over Iran,” *Journal of Hydrology*, vol. 399, no. 3-4, pp. 422–433, 2011.
- [51] T. B. M. J. Ouarda, C. Charron, K. Niranjan Kumar et al., “Evolution of the rainfall regime in the United Arab Emirates,” *Journal of Hydrology*, vol. 514, pp. 258–270, 2014.
- [52] A. R. Tomé and P. M. A. Miranda, “Piecewise linear fitting and trend changing points of climate parameters,” *Geophysical Research Letters*, vol. 31, no. 2, p. L02207, 2004.
- [53] A. N. Pettitt, “A non-parametric approach to the change-point problem,” *Applied Statistics*, vol. 28, no. 2, pp. 126–135, 1979.
- [54] G. Villarini, F. Serinaldi, J. A. Smith, and W. F. Krajewski, “On the stationarity of annual flood peaks in the continental United States during the 20th century,” *Water Resources Research*, vol. 45, no. 8, article W08417, 2009.
- [55] C. Rougé, Y. Ge, and X. Cai, “Detecting gradual and abrupt changes in hydrological records,” *Advances in Water Resources*, vol. 53, pp. 33–44, 2013.
- [56] M.-N. Yang, Y.-P. Xu, G.-B. Pan, and L.-F. Han, “Impacts of urbanization on precipitation in Taihu Lake basin, China,” *Journal of Hydrologic Engineering*, vol. 19, no. 4, pp. 739–746, 2014.



Hindawi

Submit your manuscripts at
www.hindawi.com

